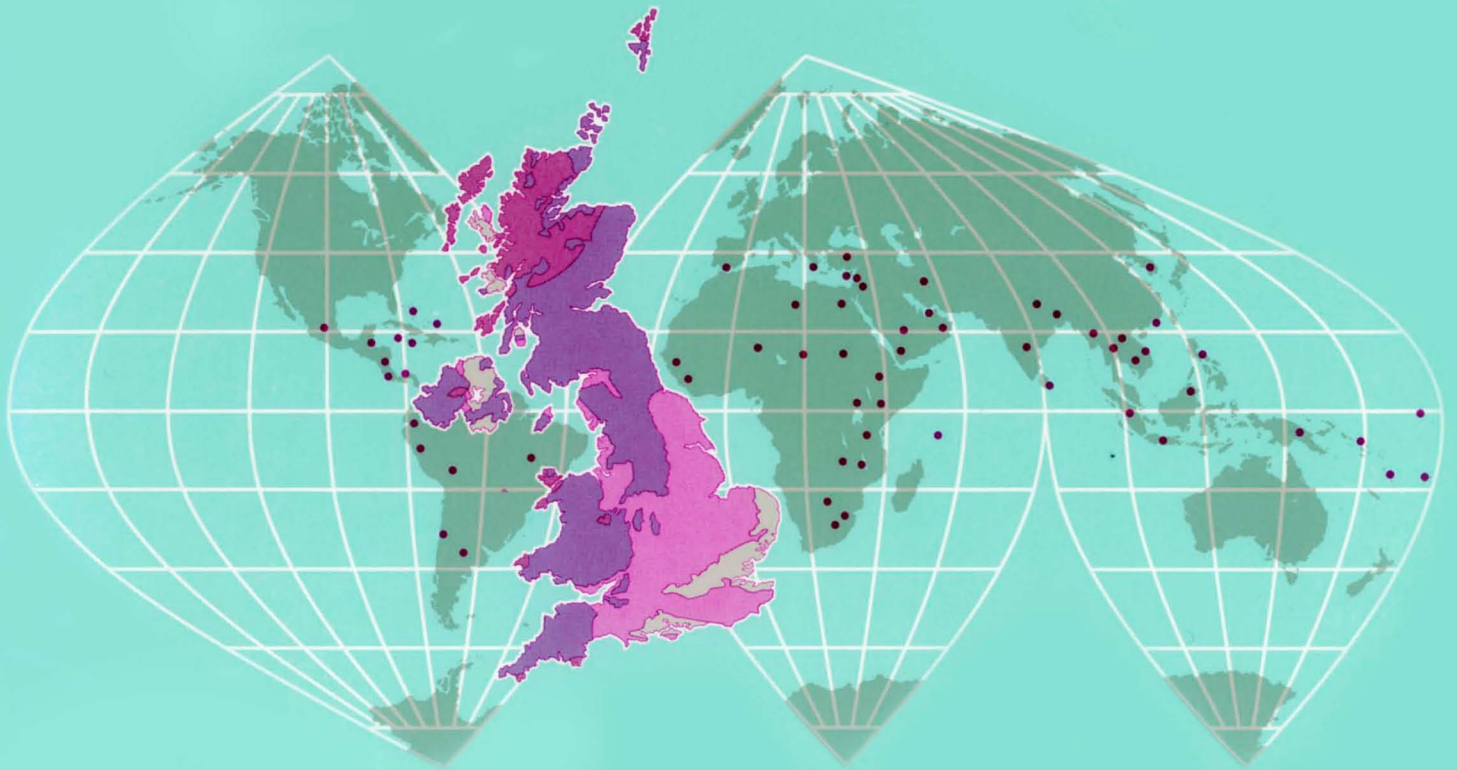


BGS Report  
Vol. 16, No. 9

BRITISH GEOLOGICAL SURVEY



## Geology, petrology and geochemistry of Ailsa Craig, Ayrshire





BRITISH GEOLOGICAL SURVEY

Natural Environment Research Council

BGS Report  
Vol. 16, No. 9

**Geology, petrology and  
geochemistry of Ailsa Craig,  
Ayrshire**

**R. K. Harrison, P. Stone, I. B. Cameron,  
R. W. Elliot and R. R. Harding**

with contributions by

**M. Brook, A. E. Davies, E. C. Hunt,  
T. K. Smith and M. T. Styles**

© Crown copyright 1987  
First published 1987

ISBN 011 884362 1

London Her Majesty's Stationery Office 1987



## CONTENTS

### Summary 1

### Introduction 2

Historical background and economic development 2

Previous geological work 4

Physiography and glacial history 4

Ailsa Craig: regional setting 7

Jointing in the microgranite 9

### Microgranite 10

Petrography 10

General description 10

Drusy structures 10

Xenoliths 12

Microscopic characters 12

Mineralogy 13

Quartz 13

Feldspar 13

Amphibole 13

Pyroxene 14

Aenigmatite 15

Minor constituents 15

Modal analyses 16

Chemistry 17

Major elements 17

Trace element geochemistry 18

Isotopic age determination 20

### Basic dykes 20

General description 20

Petrography 21

Olivine-dolerites 21

Olivine-basalts 21

Olivine-poor dolerites 22

Crinaitic dolerites 22

Mineralogy 23

Primary minerals 23

Olivine 23

Plagioclase 23

Clinopyroxenes 23

Spinels 24

Late stage and secondary minerals 24

Chemistry 24

Major elements 24

Trace element geochemistry 26

Metamorphism 26

### Discussion 26

Petrogenesis 26

### Acknowledgements 27

### References 27

**Appendix** Froth flotation of microgranite samples for precious metals 29

## FIGURES

- 1 The distribution of glacial erratics from Ailsa Craig 5
- 2 Rose diagrams showing the attitude of sub-vertical joints in the microgranite 6
- 3 Range of pyroxene compositions in eight microgranite samples from Ailsa Craig 14
- 4 Normalised rare earth plots for microgranites and basic dykes 19
- 5 Rb and Sr ratios and an isochron for the Ailsa Craig microgranite 20

## PLATES

- 1 Ailsa Craig: aerial view from the south, with the Holy Island intrusion in the far distance D2020 1
- 2 1930's views of Ailsa Craig (taken by Dr T. J. Dollar) 3
  - a Typical tools used for working curling stone 'cheeses'
  - b A boat-load of visitors to Ailsa
  - c Loading blocked-out curling-stone 'cheeses' after rolling them to the sea edge from the curling-stone quarry
  - d Mr James Girvan, now deceased, rolling a blocked-out curling stone to the foreshore for transport by boat
- 3 Recent views of Ailsa Craig 8
  - a 'Rotten Nick'
  - b Raised beach with strand-lines and hooked spit of present storm-beach
  - c 'Little Ailsa'
  - d Raised beach microgranite boulders and cobbles
  - e Very deeply denuded 'chimney' along a dolerite dyke
  - f Water-worn cave
- 4 Photomicrographs of microgranites (a–g) and a dyke (h) 11
  - a Turbid alkali-feldspars
  - b Drusy aegirine
  - c Drusy quartz
  - d Fluorite inclusions in riebeckitic arfvedsonite
  - e Pseudomorph after possible olivine, in spotted microgranite
  - f Metasomatised xenolith of pelitic siltstone
  - g As for (f), but higher magnification
  - h Olivine-dolerite (tholeiitic), with subophitic texture

## TABLES

- 1–6 Electron microprobe analyses of microgranite
  - 1 Minerals in xenolith 12
  - 2 Riebeckitic arfvedsonite 14
  - 3 Pyroxenes 14
  - 4 Aenigmatite 15
  - 5 Magnetite 15
  - 6 Glauconite-celadonite 16
  - 7 Modal analyses of microgranite 17

|                      |  |    |
|----------------------|--|----|
| 8                    | Whole-rock major element analyses of microgranite    | 17 |
| 9                    | Norms of microgranites                               | 18 |
| 10                   | Neutron activation analyses of microgranites for REE | 18 |
| 11                   | Spark-source mass spectrographic analyses            | 19 |
| 12                   | Rb, Sr and Rb-Sr-isotope values of microgranite      | 20 |
| 13–17                | Electron microprobe analyses of basic dykes          |    |
| 13                   | Olivine  | 22 |
| 14                   | Feldspars  | 22 |
| 15                   | Clinopyroxenes                                       | 23 |
| 16                   | Spinels  | 24 |
| 17                   | Late-stage/secondary minerals                        | 24 |
| 18                   | Whole-rock major element analyses of basic dykes     | 25 |
| 19                   | Norms of basic dykes                                 | 25 |
| 20                   | Trace elements of basic dykes                        | 25 |
| 21                   | Neutron activation analyses of basic dykes for REEs  | 26 |
| MAP (In back pocket) |  |    |

*Bibliographical reference*

HARRISON, R. K., STONE, P., CAMERON, I. B., ELLIOT, R. W. and HARDING, R. R. 1987  
 Geology, petrology and geochemistry of Ailsa Craig, Ayrshire. *Rep. Br. Geol. Surv.*, Vol. 16, No.9

*Authors*

R. K. Harrison\*, MSc, P. Stone, BSc, PhD, I. B. Cameron†, BSc, R. W. Elliot†, BSc and R. R. Harding\*, BSc, DPhil, FGA.

*Contributors*

M. T. Styles\*\*, BSc, PhD, A. E. Davies§, BSc, T. K. Smith§, BSc, M. Brook§, BSc and E. C. Hunt\*\*, BSc.

\* 27 Springfield Park, Twyford, Berkshire  
 RG10 9JG

† British Geological Survey, Murchison House,  
 West Mains Road, Edinburgh EH9 3LA

§ British Geological Survey, 64 Grays Inn Road,  
 London WC1X 8NG

\*\* *Formerly of the Laboratory of the Government Chemist*  
 National Physical Laboratory, Teddington,  
 Middlesex

+ British Museum (Natural History) Cromwell  
 Road, London SW7 5BD

++ British Geological Survey, Keyworth, Nottingham  
 NG12 5GG

## PREFACE

The island of Ailsa Craig is well known not only as an outstanding landmark to travellers by sea through the North Channel and Firth of Clyde, but also as the source of some of the world's finest curling stones. It is famous geologically as the origin of 'marker' erratics found in glacial deposits over wide areas around the Irish Sea. Though Ailsa Craig is so familiar a feature, no detailed study has previously been published, despite visits by geologists to the island on numerous occasions. Landing can be very difficult and access to much of the island is hazardous, especially on the western upper parts which are very steep and often slippery; of the other dangers to the visitors, not the least is that of falling debris from the vertical cliffs forming the southern and western coastline.

P. Stone, I. B. Cameron, R. W. Elliot and R. K. Harrison were responsible for the field observations and the 1:2500 survey; R. W. Elliot, R. K. Harrison and R. R. Harding described the petrography of the rocks; M. T. Styles analysed by electron microprobe the basic dykes; chemical analyses were provided by A. E. Davies, E. C. Hunt and T. K. Smith, and isotopic data by Maureen Brook.

We are most grateful to the Marquess of Ailsa and his Factor, Mr D. G. Gray, FRICS, and the Tenant, Mr I. Girvan, for permission to visit the island and collect samples. The assistance of the Northern Lighthouse Board and their keepers at the Ailsa Lighthouse is greatly appreciated.

G. INNES LUMSDEN, FRSE

*Director*

*British Geological Survey*

*Keyworth*

*Nottingham NG12 5GG*



# Geology, petrology and geochemistry of Ailsa Craig, Ayrshire

R. K. Harrison, P. Stone, I. B. Cameron, R. W. Elliot and R. R. Harding

## SUMMARY

Ailsa Craig, a prominent feature in the Firth of Clyde, is formed principally of arfvedsonite-aegirine-microgranite intruded by vertical dyke swarms of tholeiitic to alkaline (crinanitic) olivine-dolerite with basaltic margins. The dykes tend to follow the major joint-patterns in the microgranite, with three main distribution modes at the north-west, NNW and north-east. There is a quaquaversal low-angle floor-jointing. The intersections of the joint planes produce the pseudo-columnar structures in the microgranite which have been confused with a cooling-induced joint pattern. There are two types of microgranite: leucocratic, microcrystalline and sparingly feldspar-microphyric; and dark-spotted, very drusy with colour index up to 25%. The druses tend to be lined with platy arfvedsonite, feldspar and (in places) acmite or aenigmatite, and filled with later quartz. Fluorite blebs are common in the ferromagnesian minerals. Xenoliths of pelitic siltstone have been metasomatised with the development of a yellow mica and arfvedsonite. Other xenoliths include metaquartzite and silty hornfels. Apart

from texture, there is no significant mineralogical or chemical difference between the leucomicrogranite and the spotted drusy variety and the intrusion is essentially homogeneous. The finer leucomicrogranite which forms much of the upper and north-east parts of the island, may represent a near-contact facies. Microprobe analyses are given of the main minerals; accessories include magnetite, fluorite, pseudomorphs after possible olivine, glauconite, zircon, monazite, tourmaline, rutile, pyrite apatite and brookite. No gold was discovered. With the exception of higher silica, there is some chemical and mineralogical relation to the Holy Island (Arran) trachyte, and there may be a cogenetic relation to it. The trace elements are light rare-earth elements (LREE)-enriched with a marked negative Eu anomaly, indicating alkali feldspar fractionation. A relative enrichment in Zr recalls that of the Rockall aegirine-riebeckite-granite. However, the major-element chemistries differ markedly between the Rockall and Ailsa granites with a subaluminous and Fe-enrichment signature of the former.

An Rb/Sr isochron of the Ailsa microgranite indicates



**Plate 1** Ailsa Craig: aerial view from the south, with the Holy Island intrusion in the far distance

an age of  $61.5 \pm 0.5$  Ma which is the oldest recorded age of any acid intrusion in this province. The initial  $^{87}\text{Sr}/^{86}\text{Sr}$  ratio of  $0.7028 \pm 0.0009$  is extremely low for an acid igneous rock and suggests derivation through fractional crystallisation of an undersaturated mantle derivative.

The basic dyke swarm is predominantly olivine-dolerite with basaltic contacts, locally olivine-poor but also in places distinctly more alkaline (crinanitic) with accessory analcime and other zeolites. However, all are comagmatic, and chemical analyses of the olivine-dolerite compare with olivine-tholeiites.

## INTRODUCTION

The island of Ailsa Craig, situated at  $55^{\circ} 15' \text{N}$ ,  $5^{\circ} 06' \text{W}$ , 16 km west of Girvan and 20 km south of Bennan Head, Arran, forms an imposing feature in the approaches to the Firth of Clyde (Plate 1). Administratively it is a part of the Kyle and Carrick District of Strathclyde Region. It is a small, precipitous island approximately 1.2 km in diameter with cliffs rising steeply from the sea to a summit at about 340 m above OD. The cliffs are the nesting site of the myriad sea birds for which Ailsa Craig is famous. Huge colonies of gannets are concentrated onto the highest cliffs at the western and southern coasts of the island whilst guillemots, razorbills, kittiwakes and a variety of other species are ubiquitous. Geologically and petrologically the island is significant as it is composed mainly of a relatively rare rock type, alkali-rich microgranite, with the conspicuously dark accessories arfvedsonite and acmite. Related rocks of peralkaline affinity include the aegirine-riebeckite granite of Rockall Island and the Lundy Island granite. Nearer to Ailsa Craig the Holy Island off Arran, although a riebeckite-trachyte, is chemically distinct in several respects. Silica-unsaturated alkali rocks are also rare in the UK but do include the nepheline-phonolites of the Wolf Rock, Cornwall, the Bass Rock in the Firth of Forth and Traprain Law in East Lothian. The alkaline rocks forming all of these minor intrusions are characteristically of great strength and chemical stability and hence have resisted erosion to form prominent topographic features, even in such an exposed situation as Rockall in the north Atlantic. These qualities in the Ailsa Craig microgranite have also led to its popularity as a curling stone and perhaps partly explain the survival of erratics through considerable glacial transport, two phenomena associated with Ailsa Craig which have ensured the wide distribution and renown of its microgranite.

## HISTORICAL BACKGROUND AND ECONOMIC DEVELOPMENT

Much of the following summary is abstracted from the Rev. R. Lawson's (1895) account of the history of Ailsa Craig. The name, Ailsa, is of Celtic origin and is probably derived from *Aill*, a cliff, and *a*, an island, hence Rocky Isle. It is now inhabited only by the lighthouse keepers but has, in the past, supported a larger and more varied population as evinced by the ancient castle and other ruins.

By late medieval times Ailsa Craig was a part of the Barony of Knockgarron, itself included in the domains of the Carrick Earls of Turnberry Castle. One of the principal resources of the island was the large population of sea birds which were 'harvested' to help provide for the Abbey of Crossraguel nearby on the mainland. During the religious conflicts of the late 16th century the strategic

importance of Ailsa Craig, commanding the entrance to the Firth of Clyde, led to its garrisoning and fortification. This was primarily in response to an attempt to seize the island by Barclay of Ladywood, who was apparently thwarted by the Rev. Andrew Knox. The castle was then built on the orders of the Earl of Cassillis by Thomas Hamilton whose coat of arms may still be seen on its walls. After the Reformation Ailsa Craig came formally into the possession of Cassillis who, in 1850, was created Marquess of Ailsa. In 1883 the five-acre area of raised beach on the east coast of the island was sold for the erection of the present lighthouse.

For the last century at least Ailsa Craig has been variously used as a base for fishing, for grazing goats, rearing pigs (*note*, 'Swine Cave'), harvesting sea birds and their eggs and catching rabbits. The Rev. Lawson noted the presence on the island of some 80 goats, abundant rabbits and slow-worms. Shipborne rats, previously numerous, were almost extinct at the time of his visits. Rabbits are still prolific but none of the other animals was seen during the 1980 and 1983 geological visits although several grey seals were observed hauled up on the beaches in June 1980.

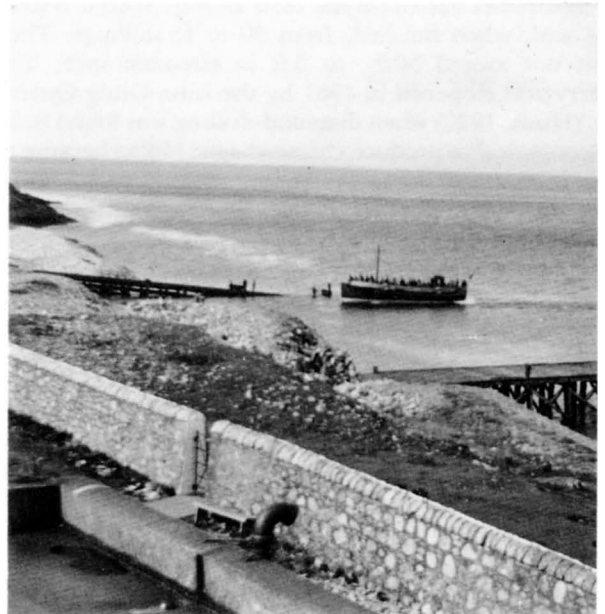
The Marquess of Ailsa leased the island to a tenant who paid a yearly rent from the sale of rabbits and the export of curling stones. Originally the tenant's cottage stood near the jetty and there are also records of an adjacent chapel and cemetery, but in about 1845 the site was cleared to allow the building of a row of fisherman's cottages. These were associated with a project to supply fish to Glasgow and Liverpool but the leader of the enterprise died and the houses were dismantled. Subsequently the site was used for gasworks and two gasometers which supplied fuel for the lighthouse and foghorn compressor. The two foghorns, one at the north and one at the south of the island were completed in 1886. They were blown by compressed air fed through slots in a revolving barrel and were said to have a range of 20 miles. Both are now disused and have been replaced by modern equipment at the lighthouse. The latter is 7.6 m high and shows six white flashes in 15 seconds followed by a 15-second interval.

Tourist visits to Ailsa Craig have declined markedly since the end of the last century when the Rev. Lawson recorded 200 people landing on one day with approximately 1000 over the whole year. The main attraction, apart from the bird life, is the climb to the summit cairn with the reward of superb views in clear weather over the Clyde, Ayrshire coast, Kintyre and beyond. However, there are no facilities for tourists, the crossing from Girvan can only be made in certain weather conditions and landing is possible only from small boats at high tide. The pathway to the castle is in places narrow and with a steep slope to seaward it is not recommended to visitors prone to vertigo.

The economically most significant and world renowned resource of the island has been the working of particular facies of the microgranite for curling stones (Plate 2, c-d). The texture of the microgranite varies from dense microcrystalline and microphyric to a somewhat coarser vughy rock with prominent dark patches of ferromagnesian accessories. The fine-grained lithology is the toughest and hardest type taking the highest polish and so this microgranite has been the most worked for curling stones on the north-east coast. The Rev. Lawson notes that in the 1870's some 50 pairs of curling stones were exported annually, whereas in the 1890's this figure rose to 1000 pairs. There were 'red' and 'blue' varieties, the former being rarer and thus preferred. He noted that a pair of



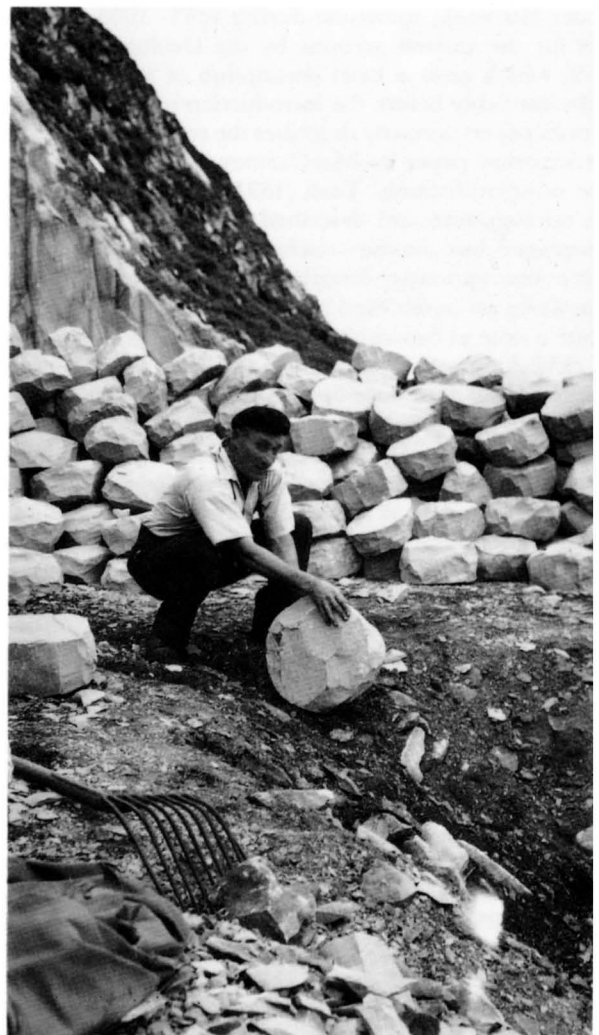
a



b



c



d

**Plate 2** Historic views of Ailsa Craig taken in the 1930's by the late Dr A. T. J. Dollar:  
**2a** Typical tools used for working curling stone 'cheeses'  
**2b** A boat-load of visitors to Ailsa

**2c** Loading blocked-out curling-stone 'cheeses' after rolling them to the sea-edge from the curling-stone quarry (NE side)  
**2d** Mr James Girvan, now deceased, rolling a blocked-out curling-stone to the foreshore for transport by boat.

blocked stones varied (in the 1890's) from 3s 6d to 9 shillings and, when finished, from 30 to 45 shillings. They must not exceed 50 lb, or 3 ft in circumference. The quarry was reopened in 1961 by the Ailsa Craig Quarry Co. (Hush, 1970) when diamond-drilling was found to be uneconomical to produce cheese-shaped blocks because of wear of the machine tools (Anon., 1961). Despite resorting to hand-working, the enterprise remained uneconomic and closed in 1973.

The microgranite has also been worked, mainly along the south coast, for a wide variety of building purposes, including granite setts for Glasgow and other centres, ornamental stone (as for the National War Memorial, Edinburgh Castle; the memorial cairn to William Wallace and Robert Burns in Leglen Woods on the banks of the R. Ayr; and in Thistle Chapel, St. Giles Cathedral, Edinburgh). Small ornaments were worked as a by-product of the curling stone industry.

#### *PREVIOUS GEOLOGICAL WORK*

No systematic geological and petrological survey of Ailsa Craig has previously been published despite initial surveys by such eminent geologists as Sir Archibald Geikie. His work, sometime during 1863–1865, was the basis for the earliest account by the Geological Survey (1869) which gives a brief description of the island but (understandably before the introduction of the polarising microscope) erroneously describes the rock as 'syenite'. A contemporary paper by MacCartney (1869) contains the same misidentification. Teall (1891) recognised the rock as a microgranite and described riebeckite and general petrography but another confusion arose from Lawson (1895) who variously described the main rock type of Ailsa Craig as 'basalt' and 'syenite greenstone'. This was despite a note in Lawson's paper by Geikie that it was in fact riebeckite-microgranite intruded by vertical dykes of dolerite. Gold was supposedly discovered in the grey microgranite by James Blackwood and supposedly confirmed by Heddle (1897) who described it as 'minute specks up to 0.006 mm across'. However, re-examination (by R.K.H. and R.W.E.) of Blackwood's thin sections did not substantiate this identification and it is probable that metallic (? pyritic) microinclusions in vughy quartz were mistaken for gold. In the early 1920's Peach and Horne revised Geikie's original survey but little further mineralogical work emerged until the studies by Meighan (1979), and Howie and Walsh (1981). The former's investigation of the acid rocks of the British Tertiary Province provided new data on trace elements in the Ailsa Craig microgranite whereas the latter refined the identity of the ferromagnesian minerals as riebeckitic arfvedsonite and aenigmatite.

#### *PHYSIOGRAPHY AND GLACIAL HISTORY*

Lawson (1895) likened the distinctive profile of Ailsa Craig to a huge sugar loaf or tea cosy. This prominence is due to its height (339.5 m, 1114 ft) combined with the steepness of its sides especially on the north, south and west coasts (Plate 1). The steepness is emphasised when the height is compared to the overall surface dimensions: 1.3 km from north to south, 1.15 km maximum east to west, a circumference of about 2.6 km and an area of 494.2 hectares. The precipitous cliffs are primarily the results of marine erosion but the initiation of a strongly positive topographic feature associated with the microgranite intrusion probably occurred during glaciation. The resistance of the microgranite to erosion compared to the response of the soft Permo-Trias sandstones

into which it is intruded was then of crucial importance. Some idea of the principal, southward, direction of ice movement is shown by the slight broadening of the island from north to south, albeit that this outline has been considerably modified by later marine action. The tough microgranite also survived well during transport as glacial erratics and, being a distinctive rock type, can readily be observed in till deposits; Figure 1 shows the localities from which erratics of Ailsa Craig microgranite have been collected (summarised by Charlesworth, 1957). The first discovery was made in the Isle of Man (Kendall, 1891) and subsequently a wide distribution of erratics was recorded from Pembrokeshire (Jehu, 1904) to Donegal (Corkey, 1937). The pattern illustrates the flow directions of the two interfering ice sheets which, at various times, have crossed the island. The dominant influence was ice originating in the Scottish Highlands and flowing south and south-west. However, at times ice emanating from the Southern Uplands and flowing north-west has carried erratics into Kintyre and the north of Ireland (Figure 1). Doubtless many of the erratics came to their final resting place by extremely devious routes.

By comparison with the erosive history, glacial deposition on Ailsa Craig is extremely minor in character. Rounded vein-quartz pebbles up to 2.5 cm across and rounded, very altered lava pebbles were found below Castle Well.

No erratic boulders or till deposits were observed during the recent geological survey but historical accounts seem convincing evidence for more widespread till deposits. MacCartney (1869) described a pocket of boulder clay at a height of about 600 ft, on the north side of the island, as a red, sandy clay containing large, striated pebbles of quartz, 'metamorphosed sandstones' and a 'clay nodulite' derived from shale. The red colour was subsequently thought by the Boulder Committee (1884, p. 791) of the Royal Society of Edinburgh to be derived from the Old Red Sandstone rocks of the Arran area but, since the Ailsa Craig microgranite is intruded into red Permo-Trias sandstones, these latter seem a more likely source for the red, sandy matrix of the till. Also, regolith from reddened dyke/microgranite contacts may have contributed. Additional erratics of quartz and granite were also recorded by the Boulder Committee with the strong implication that these were from localities other than the red boulder clay exposure. One of these granite erratics may have been re-discovered by Vevers (1936) who noted 'a large granite boulder obviously contorted' at about 850 ft to the north of Garry Loch, but from his description this could possibly be a boulder of gneiss.

Post-glacial processes have also been responsible for both erosion and deposition. The spectacular sea cliffs on the north, south and west of the island are the product of marine erosion although for the most part the cliff foot is now about 5 to 10 m above sea level and so marks a raised shoreline. In plan view the island is made markedly asymmetrical on the east coast by another abandoned feature, a triangular spread of raised beach (Plate 3d) fringed by prograding storm ridges and an associated spit (Plate 3b). This distribution of features must in large part have been caused by prevailing westerly winds and waves throughout post-glacial times. The old sea cliffs, up to 150 m high, now truncate more gentle (sloping at approximately 20°) upper slopes (Plate 1) which, if projected to sea level, suggest a more symmetrical early post-glacial profile with the north-south ratio of height: length of about 0.3 and an east-west ratio of height: width of about

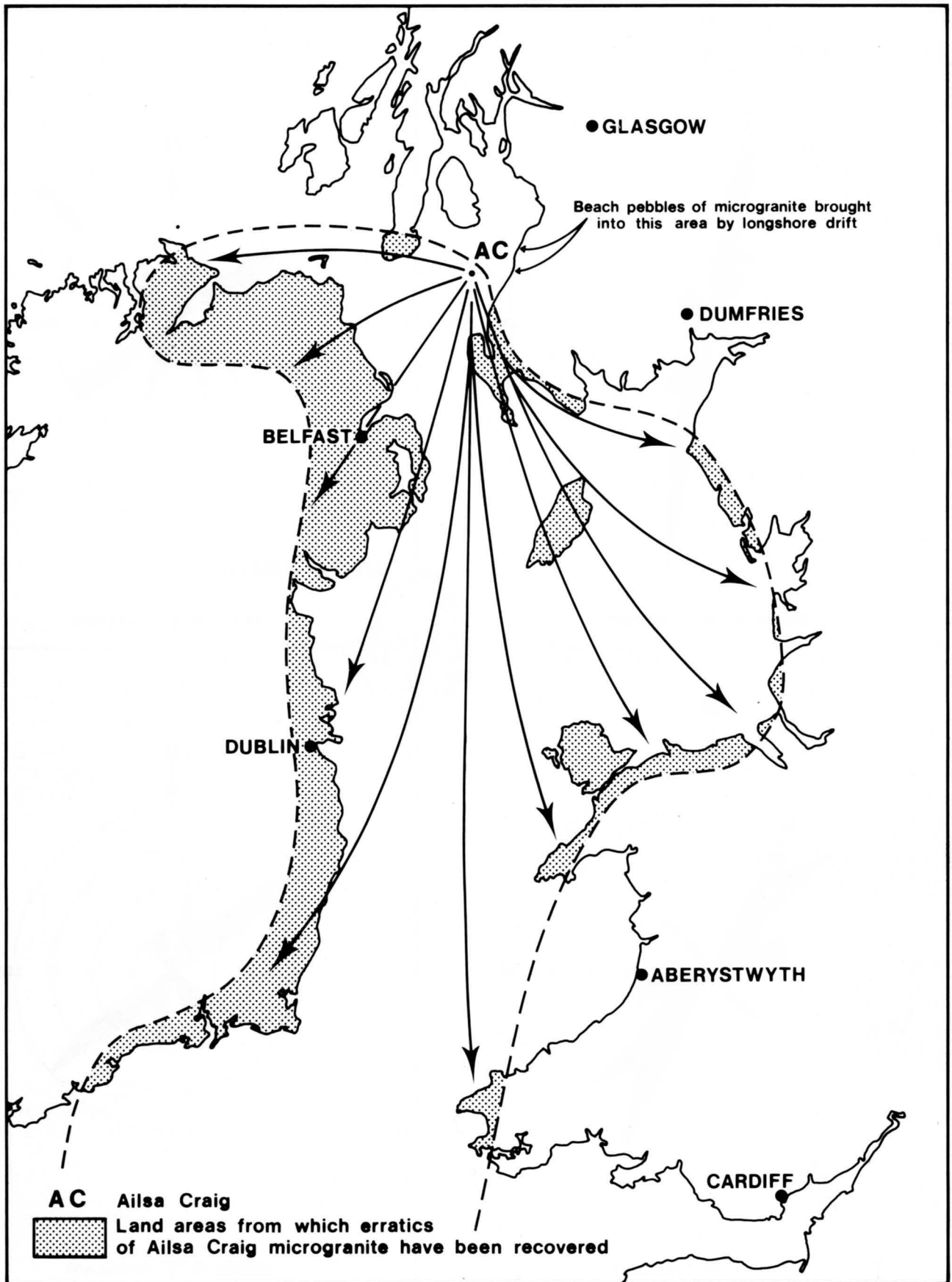


Figure 1 The distribution of glacial erratics from Ailsa Craig.

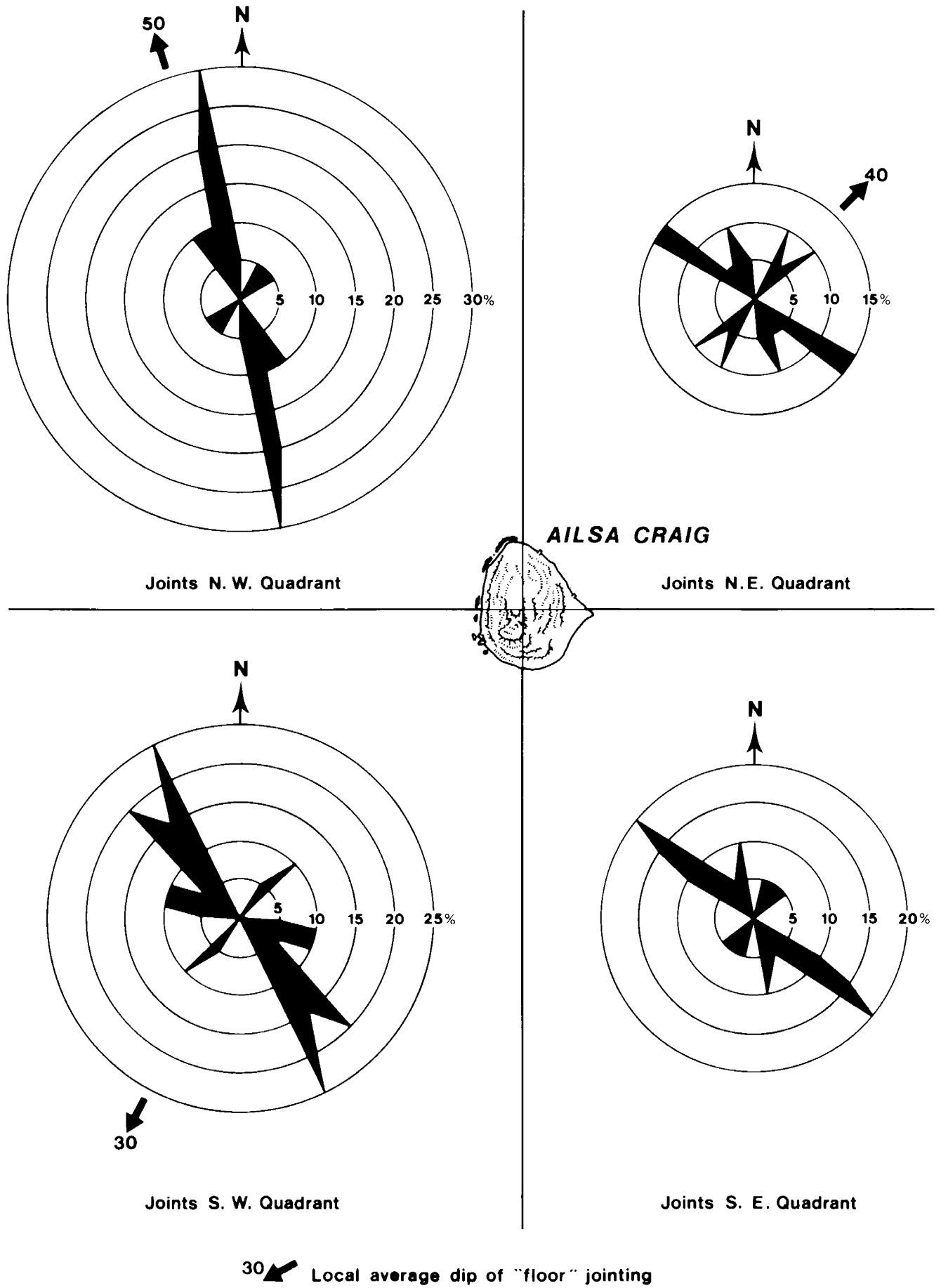


Figure 2 Rose diagrams showing the attitude of subvertical joints in the microgranite.

0.4. Despite the extent of marine erosion these gently sloping upper slopes distinguish Ailsa Craig from more exposed granite intrusions such as Rockall Island where the upper slopes (excluding the faulted east face) are inclined at 45° or more. A point of similarity is an overall convex profile resulting in prominent shoulder-like forms. Clearly such acid intrusions are exceptionally resistant to erosion, Rockall Island being an extreme case in that it is exposed to 3000 km of prevailing westerly seas and storms. Ailsa Craig is exposed to only 60 km of open sea reach south-westward to the North Channel but otherwise receives some protection from Ireland and Kintyre.

Erosion of Ailsa Craig has been facilitated by the extensive development of pseudo-columnar, sub-vertical jointing, especially on the western and southern coasts (Plate 3a) and by the presence of readily eroded basalt dykes cutting through microgranite (Plate 3e, f). The distribution of jointing has doubtless influenced the contrasting cliff development to the east and west of the island, the coincidence of jointing being best developed on the more exposed coasts compounding the erosive effects. Thus, on the sheltered east coast, with jointing only weakly or impermissibly developed in a homogeneous, massive and fine-grained microgranite facies, the gentler upper slopes of the island pass down more evenly to within about 50 m of the beach. Dykes have a more ubiquitous distribution and so do not seem to have preferentially aided erosion, except of themselves, in any one part of the island. They commonly give rise to caves low in the cliffs (Plate 3f) and to well marked depressions ('slacks') ramifying across the upper part of the island and clearly visible in aerial photographs (Plate 1). Such prominent features as Castle Comb, Dalton's Cave, Rotten Nick-Black Gair and Holes and many other minor inlets are all formed in eroded basalt dykes.

The relative lack of post-glacial erosion on the eastern coast of Ailsa Craig is also evinced by the preservation of the triangular area of raised beach (the site of the present lighthouse), the degraded surface of which varies from about 7 m to 12 m above sea level. This altitude fits the local isobase of the main Postglacial shoreline formed at the maximum of the Flandrian marine transgression about 8000 years BP (Jardine, 1971; Sissons, 1974). Fine-grained microgranite pebbles and cobbles derived from the north-eastern part of Ailsa Craig form most of the raised beach and, together with other microgranite facies variants, was the only lithology observed during the 1980 survey (apart from introduced bricks and other man-made debris). However, Dr A. J. T. Dollar, in a lecture to the Royal Society of Edinburgh which was reported (Anon., 1941) in *The Scotsman* and *The Glasgow Herald* referred to '...a former strand line at about 15 ft above present high water mark...with...associated erratic pebbles'. Rare exotic material may therefore be present in the raised beach or, alternatively Dollar may have included in his observations material from the more recent prograded storm ridges and spit which fringe the raised beach, especially on its south-east side. The majority of pebbles in these features is again of the local microgranite with the fine-grained, homogeneous facies predominating, a trend particularly marked in the south end of the spit. One cobble of basalt, probably derived locally, was also found there. Rounded fragments of brick and concrete are fairly widespread whilst MacCartney (1869) reported finding 'on the shore, at the landing place, some Irish lime' (? chalk, a hard, white limestone in north Ireland) which he speculated came from a shipwreck.

The raised beach material is mostly subrounded to

rounded but the pebbles of the spit and recent storm ridges tend to be flattened and triangular in shape with low sphericity. They are also generally less well rounded than their counterparts in the raised beach which suggests that they are freshly eroded material and are not derived by reworking of the raised beach deposits. The spit is fairly mobile in response to the local north to south long-shore drift such that, between June and September 1980, a small coastal lagoon was eliminated.

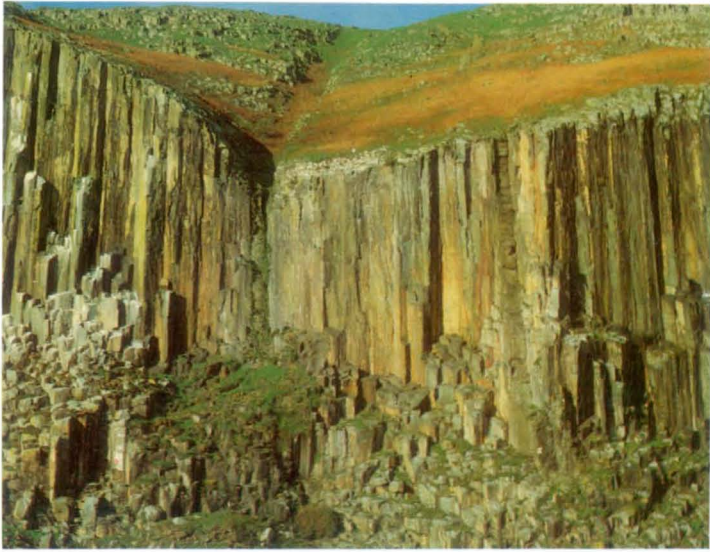
Superficial deposits at the base of some cliffs and away from the coast consist largely of frost-shattered scree. This mantles the less steep upper slopes and hollows and is concentrated into the slacks caused by the weathering of basalt dykes. With the exception of this residual regolith, eroded material falls to the shoreline and much is rapidly carried away by the sea. The largest fallen blocks, up to 7 m (20 ft) high, remain where they fall and some have acquired individual names such as Boating Stone and Ashy-doo Church.

Soils are developed in some of the slack areas along the eroded dykes and in the larger depression flooring Garra Loch, itself formed at the intersection of two major dykes (Garraloo, north-south and Ashwaun, north-east to south-west). Garra Loch, which was dry during the summer of 1980, is the major area of peat accumulation on the island, with minor peat accumulations in other slacks. It has been probed to a depth of 5 m without encountering bedrock (Lawson, 1895) and is surrounded by a luxuriant growth of moss. Other plants observed, particularly in the slacks, included bluebells (wild hyacinth), champions, bracken, stinging nettles and heather, although the latter tends to grow more on the thin soil over the granite itself. There are no trees on the island except for the scrubby elder bushes at the foot of the Trammins which, first noted by Lawson in 1895, were still growing in 1980. Those near the southern foghorn appeared to be dead in September 1983. The rankness of the flora was attributed by Lawson to the damp, windy weather and the abundant guano. However, specimens of a white substance coating microgranite beneath the granite columns have proved to be gypsum. An extensive list of plants (collected in 1844) is given by Balfour (*in* Lawson, 1895) and the vegetation is further discussed by Vevers (1936).

The steepness of slope and overall convexity of the island cause rapid rainfall run-off so that no persistent streams exist. The only catchment basin is Garra Loch which apparently is often dry in summer. However, there are reports of several springs (Lawson, 1895) including the main wells above the 'Loups' which formerly supplied houses on the raised beach, the Horse Well at the rear of the raised beach and the Castle Well above the castle; the lighthouse is supplied by these springs. Although the overall convex shape of the island might suggest radial run-off, drainage is controlled more by the slack features caused by the outcrop of differentially weathered dykes which form virtual drains to the cliffs. This factor in turn has accelerated sub-aerial erosion of the dykes.

#### *AILS CRAIG: REGIONAL SETTING*

The Ailsa Craig pluton lies within the projected limits of the Midland Valley of Scotland. The southern margin of the graben is marked by a zone of faults including the Stinchar Valley and Glen App faults, and Ailsa Craig lies on the north side of this zone projected offshore to the south-west. Evidence for continental rather than oceanic crust underlying the Midland Valley comes from fragments of gneiss in vents which are thought to be



a



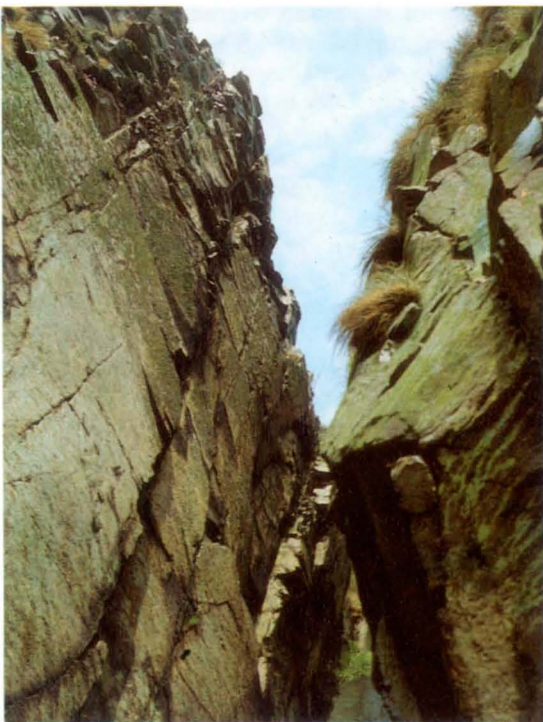
b



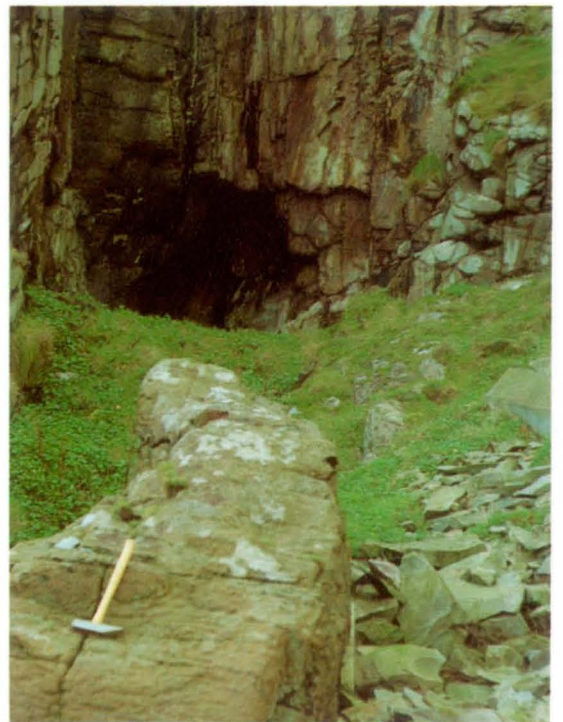
c



d



e



f

samples of the basement (Upton and others, 1976; Graham and Upton, 1978). There is also deep seismic evidence which leads to the assumption that there is continental crust at depth (Bamford, 1979). North of the Southern Uplands fault a thin and relatively undeformed sequence of Lower Palaeozoic sediments is thought to overlie the basement. Devonian and Carboniferous sedimentation was affected by repeated movement on north-easterly trending fundamental fractures. Thickness variations across faults in the Southern Uplands fault zone are considerable.

The bed of the Firth of Clyde from around Arran and Kintyre to the north Irish coast is floored with sediments mainly of Permian and Triassic age (Evans and others, 1982). The sediments occur on shore in Arran, in the Mauchline Basin, in a small outcrop at Ballantrae, around Loch Ryan and along the Antrim coast. The sediments consist of a red-bed sequence of desert sandstones, breccias and playa lake deposits. Lavas occur at the base of the sequence in the Mauchline Basin and were found at a comparable horizon in a borehole at Larne (Penn and others, 1983). Plant material in sedimentary intercalations in the lavas near Mauchline give a tentative Lower Permian age and this is extended to include the overlying dune-bedded Mauchline Sandstone (Wagner, *in* Smith and others, 1974). On Arran, beds higher in the sequence have yielded miospores of early to middle Triassic age (Warrington, 1973).

The outcrops offshore are delineated on the basis of apparent similarity with either the dune-bedded, brick-red Mauchline Sandstone or the Triassic sandstones and mudstones of south Arran.

The Ailsa Craig pluton is intruded into a broad outcrop of gently dipping rocks thought to be equivalent to the Mauchline Sandstone. A north-easterly trending fault, the Plateau Fault, crosses the area between Ailsa Craig and Arran and it has an estimated downthrow to the north-west of more than 300 m west of Ailsa Craig. Rocks similar to the Triassic on Arran are downthrown against Permian sandstone.

South of Ailsa Craig another north-easterly trending fault separates Permian sandstones from Ordovician greywackes and shales on the south-east side of the fault.

Geophysical measurements and interpretation indicate the presence of a dyke-like body of basic rock extending from Ailsa Craig north-north-westwards to Bennan Head on Arran. The feature exists as a gravity anomaly and also as a magnetic anomaly (McLean and Wren, 1978). The magnetic anomaly is a relatively shallow expression of the deeper and larger body which is responsible for the gravity anomaly. There are also small rock pinnacles on the sea bottom which are interpreted as plug-like bodies of

igneous rock emplaced as offshoots of the underlying dyke. The source of the magnetic anomaly is 0.5 km to 1 km wide.

The geophysical evidence for basic igneous rocks at depth in the vicinity of the intrusion tends to support Meighan's (1979) conclusion that the Tertiary granites formed predominantly by differentiation of basic magmas in the upper part of the crust.

Igneous activity in the British Tertiary Province was associated with a broad positive thermal anomaly which caused local updoming, and the volcanicity was coeval with the initial separation of Greenland from the Rockall Plateau and the latter from Europe. Walker (1979) postulated the presence of two or three north-westerly trending narrow thermal ridges in a region of NE-SW tension to account for the orientation of the Skye, Mull and Arran dyke swarms.

The igneous activity took place 50 to 61 million years ago and the extrusion of plateau basalt in Antrim, Mull and Skye immediately preceded or was partly contemporaneous with the formation of the plutonic centres (Macintyre and others, 1975). Individual ages for the granites on Arran are given by Evans and others (1973) and ages for the Holy Island Sill and Ailsa Craig are quoted in Macintyre (1973), but Ailsa Craig is now found to be the oldest intrusion at  $61.5 \pm 0.5$  Ma. The mean age for the plutonic complexes is stated to be 58.3 million years by Macintyre and others (1975).

#### JOINTING IN THE MICROGRANITE

Throughout the island the microgranite is cut by sub-vertical joints. These form three distinct groups with distribution modes at north-west, NNW and north-east (Figure 2) although in the north-west quadrant of Ailsa Craig the first of these sets is only weakly developed. Either the north-west or the NNW trending set is dominant in any one area but the north-east-trending joints are of great importance since their intersections with other joint planes produce the pseudo-columnar effect which, in the past, has been confused with a cooling-induced joint pattern. Thus, Lawson (1895) described the microgranite as basalt and subsequent authors drew unjustified comparison with the Giant's Causeway. However, the jointing in the Ailsa Craig microgranite does not produce regular polygonal columns; interfacial angles range between  $80^\circ$  and  $130^\circ$  and usually quadrilateral or pentagonal forms are produced. Even these may be incomplete with only two or three faces developed. The diameter of the pseudo-columns ranges up to about 2 m but the majority are 0.5 m to 1 m. Hence they form convenient sized blocks for the manufacture of curling stones and it is probably significant that the most uniform level of development of the three joint sets is found in the north-east quadrant (Figure 2) where the main quarry is situated. The attitudes of the basalt dykes intruding the microgranite are generally parallel to the joint sets with the majority of the dykes having a NNW or north-west trend. Where a mineral orientation fabric is present in the microgranite this also tends to have a sub-vertical, north-westerly-trending attitude parallel to local jointing.

Superimposed on the sub-vertical joints is a more gently dipping set (Plate 3a), poorly developed in the south-east quadrant, which is quaquaversal in dipping seaward wherever it occurs (Figure 2). The moderately dipping attitude of this 'floor' jointing governs the seaward-sloping features within and at the top of the sea cliffs and is probably important in defining the profile of the island. It has certainly facilitated marine erosion and many of the large fallen blocks at the cliff foot are joint-bound on all sides.

#### Plate 3 Recent views of Ailsa Craig

**3a** 'Rotten Nick'—a prominent slack denuded along a vertical dolerite dyke and pseudo-columnar microgranite cliffs (S. side)

**3b** Raised beach with strand-lines and hooked spit of present storm-beach

**3c** 'Little Ailsa'—an isolated mass of microgranite and dyke (not visible), resembling in shape (and petrology) the main Craig

**3d** 25 ft (7.6 m) (a.m.s.l.). Raised beach composed almost entirely of well-rounded, flattened microgranite boulders and cobbles (E. side)

**3e** Very deeply denuded 'chimney' along a dolerite dyke (SE side)

**3f** Water-worn cave denuded in a dyke at about 25 ft (7.6 m) a.m.s.l. with core of resistant dolerite in the foreground. (The Loups, NE side)

## MICROGRANITE

### PETROGRAPHY

#### *General description*

Over much of its outcrop the Ailsa Craig microgranite is microphyric, light gray (N6–N7) to yellowish or greenish grey (5GY6/1) and distinctively spotted black with variably distributed clots (up to 5 mm) of ferromagnesian minerals occupying or adjacent to drusy cavities. Feldspar microphenocrysts are common in a microcrystalline groundmass (Plate 4a). This is the distinctive lithology ('ailsyte') with which the very widespread glacially distributed fragments from Ailsa are usually matched. The other major, but less distinctive microgranite lithology is leucocratic (Colour Index less than 5), microcrystalline to saccharoidal, with feldspar microphenocrysts, sparser ferromagnesian, and drusy cavities which are much less conspicuous and smaller than in the first lithology. The leucomicrogranite (Plate 1) forms the north-east cliffs and much of the upper slopes of the Craig. The junction between the drusy black-speckled microgranite and the leucomicrogranite is probably gradual; in the eastern slopes of the Craig the junction lies along the western edge of Castle Well Combe (a prominent slack eroded along a basaltic dyke) but cannot be mapped far because of steep terrain. This gives a horizontal outcrop width of about 160 m, with the leucomicrogranite extending to the west of Nettley Howe. The western slopes are also extremely difficult of access and it was not possible to map the junction here, but it can be assumed that much of the upper part of the Craig comprises leucogranite extending to the north-eastern cliffs and forming the source of the 'blue hone' and 'red hone' stone for the past quarrying of curling stones. The significance of these two major lithologies of the microgranite is discussed below. The southern, western and north-western cliffs are all formed mainly of the spotted drusy microgranite and the distribution of the leucomicrogranite is not symmetrical with the shape of the island. Along the north-east cliff section about 375 m north-west of the jetty fine-grained leucogranite crops out to the north of the coarser variety; the relations are obscure, partly through fluxioning and heterogeneity developed in the latter. The nature and angle of contact therefore between the two facies is not apparent but is probably relatively steep. Specimens S 68614\*, S 68126, S 68150 are typical examples of the fine-grained variety, and specimens S 68121-2, S 68169 of the spotted microgranite. Since drusy cavities, which are mainly infilled, vary in concentration and size, transitional lithologies between these two major types occur, as for example specimens S 68124, S 68159. Where ferromagnesian occupying drusy cavities or as individual crystals become more concentrated, as in specimens S 68140 or S 68142, the microgranite becomes submafic with Colour Index approaching 25%.

#### *Drusy structures*

Except in the leucomicrogranite, cavities partly filled with ferromagnesian and other minerals are usually prominent, as in specimen S 68147 in which euhedral crystals up to 3 mm project into the drusy cavity. They are mainly spheroidal to ellipsoidal (like S 68148), 1 to 10 mm across, but may be extended where the rock is foliated, to 3 cm in length. Size distribution and degree of concentration are very variable. Though spheroidal cavities occur

\* Scottish Sliced Rock Collection of the British Geological Survey

sporadically, generally the druses are filled with clear, unstrained quartz which extends in optical continuity into the surrounding groundmass quartz interstitial to the feldspar mesh. Alkali feldspar extends into some druses and replacement of feldspar confirms quartz as the last-formed phase. The ferromagnesian commonly occupy or lie to one side of the drusy quartz and extend into optically-continuous skeletal poikilitic areas in the adjacent groundmass (Plate 4c). In places (such as in S 68138, S 68149) drusy patches are rimmed by feldspar and quartz.

While the term 'drusy' is particularly appropriate where cavities remain between the crystals, in many specimens original cavities have been completely filled, especially with ferromagnesian and later quartz and subordinate feldspar. Whether all of the ferromagnesian-quartz clots which characterise the spotted microgranite represent filled original pores is uncertain, but their overall resemblance to the crystal-lined druses does support that origin. Rarely, small perfectly spheroidal (? gas) cavities occur, and on a freshly broken surface contain a black, very friable substance which is probably amorphous. In the leucomicrogranite the ferromagnesian minerals are finely crystalline (up to 1.5 mm) and dispersed, and these give an overall impression of considerably finer grain than the spotted drusy microgranite. However, not all the leucogranites are distinctly finer grained. In some specimens (such as S 68178), there are abundant, small, roughly spheroidal to ellipsoidal dispersed ferromagnesian, and also cavities (up to 2 mm diameter); by analogy with the spotted microgranite these are all regarded here as drusy-type structures and are described in detail below.

Phenocrysts are generally common in the body of both microgranite lithologies, ranging up to 3 mm length and are predominantly feldspar. They are particularly prominent as white rectangular tablets in the leucomicrogranite from the old curling-stone quarries in the north-east part of the island. None of the coarser quartz appears to be truly phenocrystic, and where the drusy occupancy is uncertain, the non-committal term 'microcryst' is used.

#### **Plate 4** Photomicrographs of microgranites (a to g) and a dyke (h)

**4a** Turbid alkali-feldspars, with dominant low-albite and lesser orthoclase. Below Black Gair (SW side)  
S 68169 Crossed polarisers  $\times 80$

**4b** Drusy aegirine charged with fluorite blebs and bordering euhedral fluorite.  
S 68121 West side Uncrossed polarisers  $\times 220$

**4c** Drusy quartz mantled by riebeckitic arfvedsonite and in turn by aegirine (pale brown) in leucomicrogranite.  
S 68124 NW side Uncrossed polarisers  $\times 133$

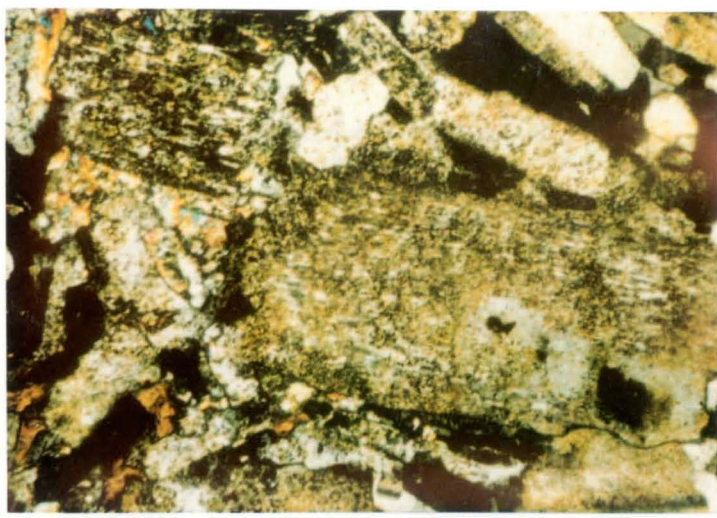
**4d** Fluorite inclusion (black) in riebeckitic arfvedsonite  
S 68179 Near top of Craig. Crossed polarisers  $\times 153$

**4e** Pseudomorph (left centre) after possible olivine, with riebeckitic arfvedsonite and feldspar, in spotted microgranite  
S 68153 NNE side Crossed polarisers  $\times 133$

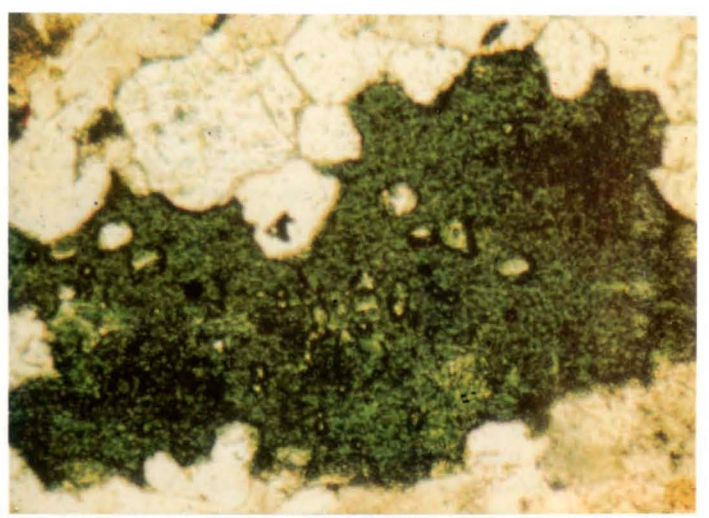
**4f** Metasomatised xenolith of pelitic siltstone showing detrital quartz grains and secondary mica. NE Curling Stone Quarry.  
S 72698 Crossed polarisers  $\times 141$

**4g** As for f, but higher magnification showing replacement of detrital feldspar (grey, centre) by secondary mica (right and lower centre)  
Crossed polarisers  $\times 360$

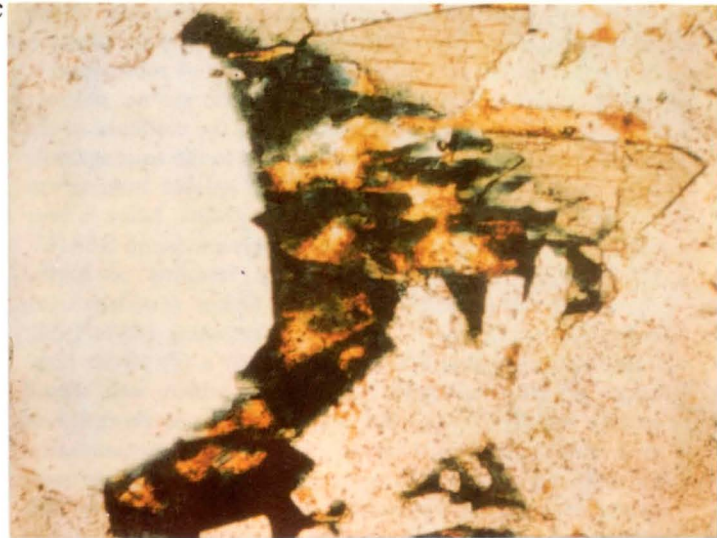
**4h** Olivine-dolerite (tholeiitic), with subophitic texture  
Centre of dyke  
S 68118 Near N. Foghorn. Crossed polarisers  $\times 80$



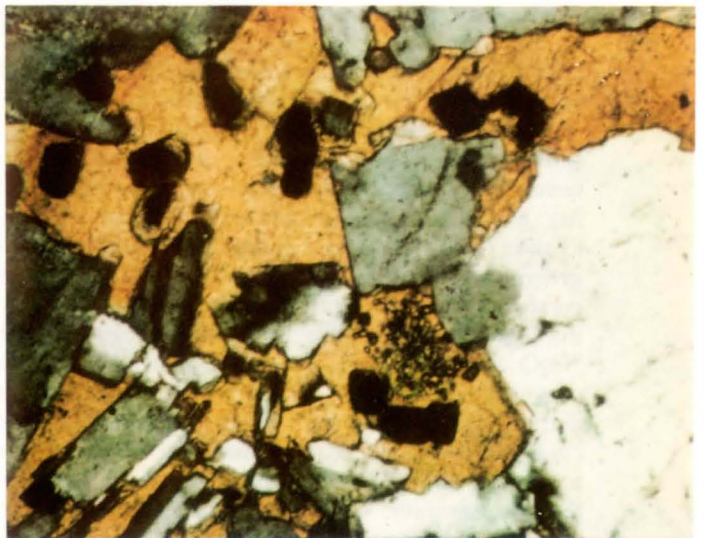
a



b



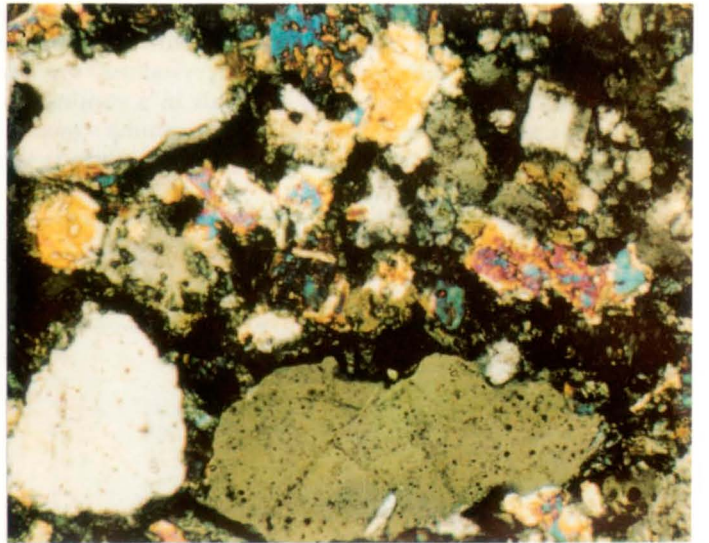
c



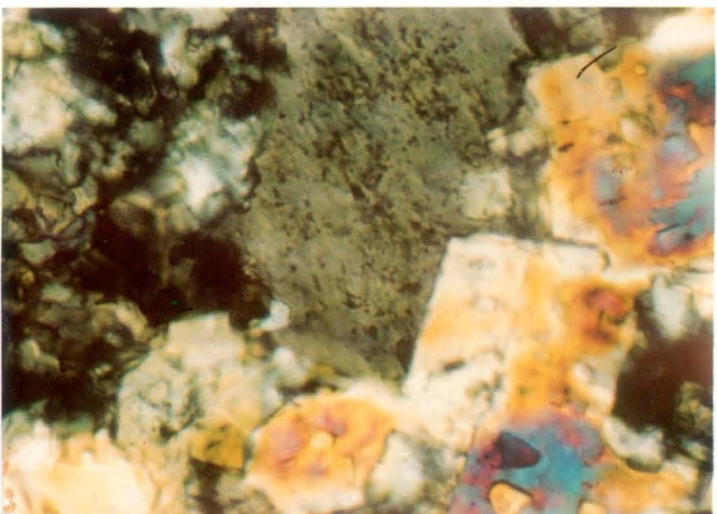
d



e



f



g



h

### Xenoliths

Xenoliths of metasedimentary rocks occur sporadically. Small xenoliths up to 2 cm across were found in 1983 in the remains of blocks cored for curling stone, near the north-east quarry. These suggest polygonal outlines emphasised by a dark rim of arfvedsonite crystals. Thin sections (S 72698 A,B) show the xenoliths to be composed of rounded to marginally etched detrital quartz grains of moderate sphericity, averaging 0.2 mm diameter, with secondary overgrowths, abundant alkali feldspar of similar grain size, heavily altered to dusty secondary clay and with clear overgrowths, blue-green amphibole, yellow mica (0.1 mm) with pleochroism: X = colourless, Z = reddish yellow and fragments of darker, finer-grained micaceous material (Plate 4f, g).

Electron microprobe analyses of some xenolith minerals are given in Table 1. The mica in the fine-grained fragments is biotite and is intergrown with almost pure albite. In contrast the pale yellow mica in the coarser part of the xenolith is associated in places with arfvedsonite and has the composition of a tetrasilicic mica intermediate in composition between the naturally occurring montdorite and a synthetic Mg tetrasilicic mica (Table 1, cols. 4, 5 and 6 and listed references). Blue-green arfvedsonite is abundant in microgranular crystallites; it is optically similar to that in the microgranite but differs in its higher SiO<sub>2</sub>, MgO and Na<sub>2</sub>O and lower total Fe (Table 1, col. 3). Of the accessories, colourless fluorite conspicuously replaces detrital quartz, mica and other minerals. Feldspars include albite-oligoclase, orthoclase and cryptoperthite and apparently differ little in composition from those forming the microgranite. Composite finely granular quartzose aggregates resemble siltstone. 'Leucoxenitic' dust permeates the xenoliths with specks of opaque iron oxide. The arfvedsonite concentrated along the contact of the xenolith and microgranite is finely equigranular (0.02 mm) forming chains of crystallites surrounding detrital quartz and other minerals in a continuous rim. Outside the xenolith contact granular quartz and feldspars are aligned parallel to the arfvedsonite rim.

**Table 1** Electron microprobe analyses of minerals in xenolith in Ailsa Craig granite (S 72698), with comparisons

|                                | 1     | 2     | 3     | 4     | 5      | 6     |
|--------------------------------|-------|-------|-------|-------|--------|-------|
| SiO <sub>2</sub>               | 39.40 | 68.20 | 55.48 | 56.02 | 47.31  | 51.93 |
| TiO <sub>2</sub>               | 4.09  | <0.20 | 1.02  | 1.04  | 2.44   | —     |
| Al <sub>2</sub> O <sub>3</sub> | 9.75  | 19.87 | 0.51  | 2.10  | 4.96   | 0.36  |
| FeO                            | 27.28 | 0.43  | 20.65 | 7.28  | 17.13  | 0.65  |
| MnO                            | 0.40  | 0.20  | 0.86  | 0.40  | 9.89   | —     |
| MgO                            | 5.06  | <0.20 | 7.76  | 15.95 | 4.30   | 30.19 |
| CaO                            | <0.20 | 0.30  | 2.06  | <0.20 | —      | —     |
| Na <sub>2</sub> O              | 0.87  | 10.03 | 9.51  | 1.24  | 1.02   | 0.28  |
| K <sub>2</sub> O               | 9.20  | 0.84  | 1.26  | 10.34 | 8.89   | 10.77 |
| Total                          | 96.05 | 99.67 | 99.11 | 94.37 | 100.34 | 99.48 |

Total iron listed as FeO.

Dash means not reported.

1 Biotite in fine-grained fragment in xenolith; mean of 4 analyses

2 Albite in fine-grained fragment in xenolith; mean of 2 analyses

3 Amphibole in coarser part of xenolith; mean of 2 analyses

4 Pale yellow mica in coarser part of xenolith; mean of 5 analyses

5 Natural tetrasilicic K-mica; total includes 4.4% F (Robert and Maury, 1979, p.118)

6 Synthesized tetrasilicic mica; total includes 5.30% H<sub>2</sub>O (Tateyama and others, 1974, p.198).

Analyst R. R. Harding

The pelitic siltstone xenolith has obviously suffered considerable metasomatism (or granitisation) in addition to thermal metamorphism. Some or most of the feldspar may be detrital — particularly those grains showing secondary overgrowths; on the other hand the lack of other distinction from the microgranite feldspars may suggest that some feldspar has been introduced metasomatically. The quartz grains show little alteration; they are of clear, igneous origin and contain rows of microinclusions. The pale yellow mica evidently represents thermally altered detrital clay material. Arfvedsonite has been introduced, though the reason for its concentration around the xenolith rim is uncertain except that such a contact represents a marked thermodynamic change favouring precipitation. Fluorite was evidently introduced pneumatolytically, and presumably these metasomatic introductions were facilitated by the porosity of the xenolith. The possibility remains of more intense digestion of country rock leaving little or no obvious evidence of the process. Extrapolating the evidence of the impure arenaceous xenolith described to the microgranite as a whole, some of the spheroidal quartz microcrysts might perhaps indicate sedimentary grains. Mica is very rare in the microgranite but its occurrence (as in S 68147, 68169) may represent the sparse remains of highly digested microxenolithic material. Other xenoliths were collected by Dr A. T. J. Dollar between 1933–1938. They include (slide No. A.T.J.D. 26) a (?) 10 cm fragment of grey quartzitic siltstone in which well sorted quartz silt (0.05 mm) has apparently been reorganised with interlocking grain boundaries, patchily metasomatised with strings and coarse grains of quartz, arfvedsonite, granular fluorite (commonly enclosed within the amphibole) and traces of other minerals. Another xenolith (A.T.J.D. 30) is a silty hornfels composed of abundant biotite microaugen of an acicular amphibole with quartz centres, sparse opaque iron oxide and apatite.

In addition to the concentration of amphiboles in druses, they also occur rarely along joints or veinlets as bladed aggregates.

In the vicinity of certain dykes, the microgranite is strikingly reddened through finely disseminated ferric oxide (such as S 68163 close to the 4-m thick dyke complex below East Trammings). Where dykes have been eroded away, the reddening of microgranite contacts (as at Castle Combe) is adequate evidence of their former occurrence.

### Microscopic characters

The macroscopic distinction between the spotted microgranite (and its submafic variant) and the leucomicrogranite is generally less obvious in thin sections except for the lower proportion of ferromagnesian in the last-named. However, some leucomicrogranites have the most finely crystalline groundmass of all lithologies. A typical example (S 68150) from the old curling stone quarry contains white rectangular feldspar microphenocrysts (1 to 1.5 mm) in a groundmass (Colour Index 8%) of K-feldspar and interstitial quartz (0.2 mm) with scattered arfvedsonite, sparse aegirine and fluorite. Minute druses (0.3 mm) are filled with quartz into which project radiating K-feldspar crystals. Fineness of groundmass crystallinity and concentration/size of druses (and ferromagnesian proportions which are related to the druses) apart, the microgranite lithologies are broadly similar in mineralogy. Textural differences include local fluxioning of feldspars and ferromagnesian. An example of submafic microgranite (S 68142) contains dark bluish grey (5B3/1) mafic-filled druses averaging 4 mm, in a

light grey (N7) groundmass; the overall Colour Index is 25%. Microphenocrysts of alkali feldspar ( $1.2 \times 0.06$  mm) include micropertthite. The groundmass is a fluxioned felt of quartz, orthoclase, albite-oligoclase with clear to cloudy segregations (laths averaging  $0.3 \times 0.04$  mm), skeletal arfvedsonite, aenigmatite, and aegirine, and scattered fluorite (0.18 mm). The ferromagnesian tend to be associated more with the segregations of clearer feldspars than with the cloudy grains. Drusy cavities are filled with quartz. In all samples the groundmass texture is not strictly granophyric (implying the simultaneous crystallisation of quartz and feldspar), because the quartz is interstitial to and evidently later than, the feldspar mesh; the quartz thus appears to fill the pore-like interstices between feldspar laths.

In summary, therefore, despite the macroscopic contrast between the leucomicrogranite and the other microgranites, which is principally due to the high concentration of coarser 'drusy' cavities — filled or partially filled with quartz and ferromagnesian (giving rise to the black spotted appearance) and giving a misleading impression of overall coarseness of texture — the microphenocrysts and groundmass of both lithologies are, in general, closely similar. Microphenocrysts of feldspar thus range from 1.0 to 3.0 mm length, a second generation about 0.6 mm length, and the groundmass feldspars range from 0.1 by 0.03 mm to 0.2 by 0.04 mm. While the larger plates of ferromagnesian are spatially associated with the druses, skeletal arfvedsonite, aegirine and aenigmatite occur in the groundmass, with blebby fluorite, sparse opaque iron oxide, pseudomorphs perhaps after olivine, rare biotite (representing digested xenoliths), zircon and other trace minerals. The groundmass feldspar mesh shows distinct clear and cloudy patches — the latter evidently due to submicroscopic inclusions, and the former more associated with the skeletal ferromagnesian. Also fluxioning of feldspars can occur in both lithologies. Though drusy cavities are sparser and smaller in the leucomicrogranite, nevertheless they contain the same mineral assemblage (quartz, ferromagnesian) as in the spotted and submafic microgranites. Petrogenetically, therefore, the Ailsa microgranite can broadly be considered as an entity, despite the apparent inhomogeneity suggested by the macroscopic differences.

#### MINERALOGY

The following account is based on analyses by electron microprobe of the minerals in polished thin sections of seven samples selected from the perimeter of the island, and one sample from near its geographical centre and top (330 m). Minerals were analysed using a Link Systems energy-dispersive (ED) X-ray analyser on a Cambridge Instruments Geoscan electron microprobe. An accelerating voltage of 15 kV, a specimen current of  $5 \times 10^{-9}$  amps and an electron beam focused to approximately  $5 \mu\text{m}$  were used. The microprobe can measure elements of atomic number 11 (Na) and above, and the limits of detection for each of the oxides measured are about 0.2 wt %.

#### Quartz

Quartz occurs in two main forms: as single or clustered microcrysts up to 1.5 mm across (similar in size to feldspar phenocrysts), and as fine-grained interstitial growths in the feldspar-rich groundmass. The quartz microcrysts are anhedral, unstrained, and clear, except for strings of gaseous or liquid microinclusions; specks of opaques also occur — probably pyrite which may

previously have been mistaken for gold (see p. 19). The microcrysts, some of which occupy drusy cavities, are optically continuous in places with the adjacent interstitial groundmass quartz. In foliated facies there is a crude orientation of the long axes of the larger quartz grains along the plane of fluxioning of feldspars. Unlike the feldspar microphenocrysts the quartz grains are anhedral and are clearly the products of residual crystallisation.

#### Feldspar

Alkali feldspar occurs both as tabular microphenocrysts (up to 1.3 mm across) and as stubby tablets in the groundmass where they commonly develop a trachytoidal texture. Both generations of feldspar possess compositions falling mainly in the range  $\text{Or}_{65}\text{Ab}_{35}$  to  $\text{Or}_{35}\text{Ab}_{65}$ , but compositions outside this range are not uncommon, particularly in the groundmass feldspars. Potassium and sodium-rich rims are found on both feldspar types, especially those close to druses. The plagioclase content is extremely low, with less than 2 mol % An present in 54 alkali feldspar grains analysed by electron microprobe. The wide variation in Or content results from the unmixed, micro- and cryptoperthitic state of the feldspars. Many grains show transformation twinning, a characteristic of high-low temperature inversion in alkali feldspars (Smith, 1974). The low-temperature perthitic composition is confirmed by XRD which shows that low-albite is the dominant phase, accompanied by orthoclase (chart DX 2713; R. J. Merriman, written communication.) Semi-quantitative estimates based on XRD peak intensities and normative whole rock chemistry suggest a bulk feldspar composition of approximately  $\text{Ab}_{65}\text{Or}_{35}$ . Secondary, turbid alteration of the feldspar is mostly due to the development of paragonite.

#### Amphibole

Amphibole occurs throughout the microgranite and forms anhedral, trachyophitic to poikilitic grains up to 5 mm across. Some grains have cores crowded with minute (less than 10 microns) rounded inclusions of fluorite (for example, S 68131, Plate 4d), but most are clear and are surrounded by rims of poikilitic habit enclosing euhedral laths of alkali feldspar. Ophitic or skeletal growths are usually in optical continuity with the coarser plates bordering or partially filling druses. These habits are also shown by aenigmatite and quartz. Amphibole may be moulded around clinopyroxene (S 68122) but the reverse relationship also occurs. The pleochroic couplets vary a little between specimens, the commonest being X = deep turquoise or aquamarine, Z = pale brown, yellow-brown or grey-brown; absorption is  $X > Z$ . Because of the intense absorption it was not possible to measure the refractive indices ( $\alpha, \beta$ ), but the microprobe analyses precisely identify the species.

Although the composition of the amphibole both within and between thin sections varies in minor content, analyses of 48 grains from the eight samples confirm it as riebeckitic arfvedsonite (Howie and Walsh, 1981). The mean of the analyses (Table 2) is not significantly different from that given by Howie and Walsh (1981), but some variation in the minor element contents deserves comment.  $\text{Al}_2\text{O}_3$  is consistently low and ranges from 0.4 to 1.2%.  $\text{TiO}_2$  is locally variable and generally lies in the range 0.5 to 2.0% but some grains contain up to 3.9%. Most grains contain less than 0.2% MgO but some contain up to 0.4%; CaO content is generally less than 2.5% and apparently higher Ca contents found in some grains are due to fluorite inclusions.  $\text{K}_2\text{O}$  content ranges from

**Table 2** Electron probe analysis of riebeckitic arfvedsonite from Ailsa Craig

Mean of 48 analyses from S 68124, S 68131, S 68136, S 68142, S 68155, S 68163, S 68169 and S 68179

| Wt%                            |              | Atomic proportions based on 23 oxygens |      |
|--------------------------------|--------------|--|------|
| SiO <sub>2</sub>               | 50.32        | Si                                     | 8.06 |
| TiO <sub>2</sub>               | 1.19         | Al                                     | 0.16 |
| Al <sub>2</sub> O <sub>3</sub> | 0.84         | Ti                                     | 0.14 |
| FeO                            | 31.90        | Fe                                     | 4.27 |
| MnO                            | 1.07         | Mn                                     | 0.14 |
| MgO                            | 0.07         | Mg                                     | 0.02 |
| CaO                            | 1.63         | Zr                                     | 0.05 |
| Na <sub>2</sub> O              | 8.87         | Zn                                     | 0.03 |
| K <sub>2</sub> O               | 1.39         | Ca                                     | 0.28 |
| Cl                             | 0.03         | Na                                     | 2.75 |
| ZrO <sub>2</sub>               | 0.62         | K                                      | 0.28 |
| ZnO                            | 0.28         |  |      |
| <b>Total</b>                   | <b>98.21</b> |  |      |

Total Fe as FeO

Analyst R. R. Harding

1.0 to 2.0%, but within this range the higher values are generally associated with high values of Zr and low values of Fe. Up to 1% ZnO is present in the amphiboles in 5 of the 8 polished sections examined. ZrO<sub>2</sub> is locally variable with the highest values (up to 5.9%) found in grains of poikilitic or interstitial habit. High Zr is associated with the marginally higher values of K and lower values of Fe in the amphibole, but there is no correlation with Na or Ca contents. The Zr content of the amphiboles is concentrated in the areas of residual poikilitic crystallisation but seems to be unrelated to any compositional pattern observed in associated pyroxene.

**Pyroxene**

This occurs throughout the microgranite as subhedral or interstitial deep green or yellow green grains generally less than 1 mm across. The main pleochroism is X = deep or grass green, Z = yellow with green. Analyses of 59 grains from the 8 polished sections are summarised in Figure 3 with selected analyses in Table 3. The pyroxene has less than 0.3% MgO and essentially is a mixture of the calcic and sodic end-members hedenbergite (CaFe<sup>2+</sup>Si<sub>2</sub>O<sub>6</sub>) and acmite (NaFe<sup>3+</sup>Si<sub>2</sub>O<sub>6</sub>) (Harding, 1983). The analyses indicate very variable compositions in the different samples with the most calcic (He<sub>87</sub>Ac<sub>13</sub>) in S 68179, and the most sodic (He<sub>0</sub>Ac<sub>100</sub>) in S 68124 and S 68131. The He-Ac range in each sample is shown in Figure 3 with the corresponding contents of Zr and Zr + Ti + Al. The patterns suggest that the north-east leucomicrogranite outcrop may have a smaller range of sodic pyroxenes than the rest of the microgranite, but many more samples need analysis before this can be confirmed. There is a general rise in the contents of Al, Ti and Zr with increasing proportions of the Ac molecule, but the correlation is not exact either within or between samples. Analyses of S 68155 (Figure 3) indicate two maxima of Zr content at different He/Ac ratios, and these do not correspond exactly with those found in S 68142 and S 68169. Variable contents of Zr, Ti and Al are also shown in the selected analyses in Table 3 with considerable amounts of Zr in analyses 2, 4 and 5, of Ti in

**Figure 3** Range of pyroxene compositions in eight microgranite samples from Ailsa Craig.

**Table 3** Electron probe analyses of pyroxenes from Ailsa Craig

|                                | 1             | 2             | 3             | 4             | 5             | 6            | 7            |
|--------------------------------|---------------|---------------|---------------|---------------|---------------|--------------|--------------|
| SiO <sub>2</sub>               | 52.97         | 51.23         | 52.89         | 51.03         | 50.91         | 49.46        | 47.36        |
| TiO <sub>2</sub>               | 0.80          | 0.70          | 5.76          | 0.81          | 0.24          | 0.31         | —            |
| Al <sub>2</sub> O <sub>3</sub> | 1.74          | 0.57          | 0.51          | 0.83          | 0.22          | 0.28         | 0.31         |
| Fe <sub>2</sub> O <sub>3</sub> | 30.28         | 29.24         | 26.68         | 24.15         | 21.05         | 14.50        | 3.90         |
| FeO                            | —             | 0.69          | 0.85          | 7.41          | 9.62          | 15.97        | 24.75        |
| MnO                            | 0.77          | 0.42          | —             | 0.62          | 0.67          | 0.99         | 1.06         |
| MgO                            | —             | —             | —             | 0.24          | —             | —            | —            |
| CaO                            | —             | 0.54          | 0.67          | 5.79          | 7.51          | 12.46        | 19.32        |
| Na <sub>2</sub> O              | 13.80         | 14.04         | 13.54         | 9.31          | 8.86          | 5.09         | 2.33         |
| ZrO <sub>2</sub>               | —             | 3.15          | —             | 1.22          | 1.27          | —            | —            |
| <b>Total</b>                   | <b>100.36</b> | <b>100.58</b> | <b>100.90</b> | <b>101.41</b> | <b>100.35</b> | <b>99.06</b> | <b>99.03</b> |

| Atomic proportions based on 6 oxygens |      |      |      |      |      |      |      |
|---------------------------------------|------|------|------|------|------|------|------|
| Si                                    | 2.01 | 1.97 | 1.98 | 1.97 | 2.00 | 2.00 | 1.97 |
| Al                                    | —    | 0.03 | 0.02 | 0.03 | —    | —    | 0.02 |
| Ti                                    | 0.08 | —    | —    | 0.01 | 0.01 | 0.01 | —    |
| Fe <sup>3</sup>                       | 0.86 | 0.85 | 0.75 | 0.70 | 0.62 | 0.44 | 0.12 |
| Fe <sup>2</sup>                       | —    | 0.02 | 0.03 | 0.24 | 0.32 | 0.54 | 0.86 |
| Mn                                    | 0.02 | 0.01 | —    | 0.02 | 0.02 | 0.03 | 0.04 |
| Mg                                    | —    | —    | —    | 0.01 | —    | —    | —    |
| Zr                                    | —    | 0.06 | —    | 0.02 | 0.02 | —    | —    |
| Ca                                    | —    | 0.02 | 0.03 | 0.24 | 0.32 | 0.54 | 0.86 |
| Na                                    | 1.01 | 1.05 | 0.98 | 0.70 | 0.67 | 0.40 | 0.19 |

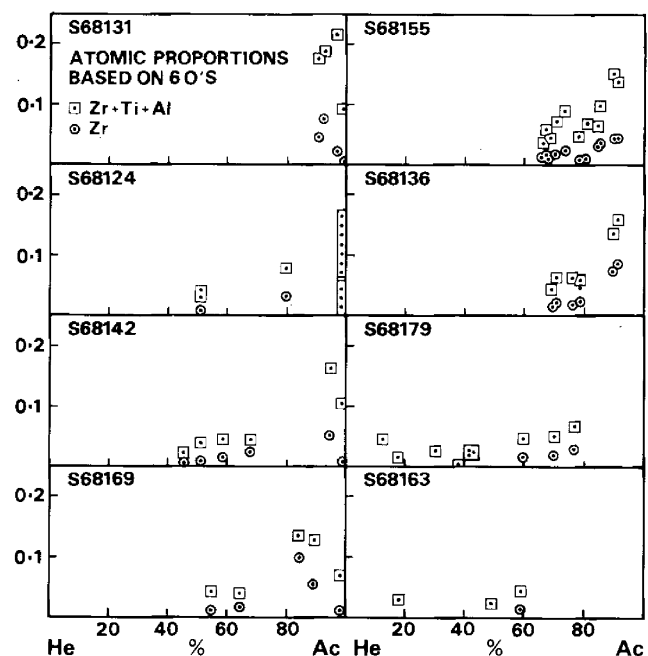
| $\frac{Na}{Na+Ca} \times 100$ |     |    |    |    |    |    |    |
|-------------------------------|-----|----|----|----|----|----|----|
|                               | 100 | 98 | 97 | 74 | 68 | 42 | 18 |

Total iron was assigned to FeO and Fe<sub>2</sub>O<sub>3</sub> on the basis of the proportions of Ac and He in the pyroxene molecule. Sufficient Fe<sup>2+</sup> was taken to balance the amount of Ca and the remainder was assigned to Fe<sup>3+</sup>.

— oxides not detected (<0.2%).

- 1 S 68124. Pale yellow pyroxene intergrown with arfvedsonite at edge of large quartz grain.
- 2 S 68124. Pale yellow green interstitial pyroxene, intergrown with brown mineral.
- 3 S 68131. Interstitial green pyroxene.
- 4 S 68155. Interstitial green pyroxene.
- 5 S 68142. Interstitial green pyroxene.
- 6 S 68179. Rim of green anhedral pyroxene with fluorite inclusions.
- 7 S 68179. Core of deep green anhedral pyroxene.

Analyst R. R. Harding



analysis 3, and of Al in analysis 1. In all cases these three elements appear to displace Fe<sup>3</sup> in the crystal structure. The variation in content of the three elements and the lack of their correspondence with particular pyroxene compositions indicate that, on a small scale, the granite was heterogeneous and that the later stages of crystallisation took place in isolated patches too far apart for diffusion to be effective.

In each sample of granite, some grains of pyroxene contain cores or zones with fluorite inclusions. Most inclusions are less than 0.005 mm across but some, especially in the outer zones of the pyroxene, reach 0.03 mm and crowd together in a sieve-like or spongy texture. Similar features are found in arfvedsonite grains, and in some samples sieve-like pyroxene cores may be mantled by arfvedsonite, with sporadic fluorite inclusions. In S 68179 analyses 7 and 6 in Table 3 are of a pyroxene core He<sub>82</sub>Ac<sub>18</sub> free of inclusions and a rim of He<sub>58</sub>Ac<sub>42</sub> with abundant fluorite grains (a similar grain is shown in Plate 4b). These textures indicate that fluorite precipitated as a shower of tiny grains after hedenbergitic pyroxene had formed but still quite early in the cooling sequence of the microgranite and suggests that the fluorine content of the magma was high. Not all of the larger grains of pyroxene contain fluorite inclusions. Some pale yellow-green grains associated with large grains of amphibole and quartz are very sodic and range from He<sub>3</sub>Ac<sub>97</sub> to Ac<sub>100</sub>.

#### Aenigmatite

Although present in six samples, aenigmatite is less abundant than pyroxene or amphibole; it forms variably pleochroic dark red-brown or opaque grains. Most grains are anhedral with poikilitic fringes enclosing euhedral alkali feldspar. The composition of the aenigmatite (Table 4) is essentially constant throughout the sampled microgranite, and there is no significant chemical variation that can be related either to crystal habit, colour, pleochroism or opacity. Analyses of aenigmatite from Ailsa Craig microgranite, carried out on mineral concentrates by wet chemical and inductively coupled plasma spectrometry (ICPS) methods (Howie and Walsh, 1981), show some variation in the Na and Ti values obtained by the two methods, and in our study the microprobe analyses of individual grains accord more closely with the (ICPS) values.

**Table 4** Electron probe analyses of aenigmatite from Ailsa Craig

|                                | 1      | 2      | 3      | 4      | 5      | 6      | 7      |
|--------------------------------|--------|--------|--------|--------|--------|--------|--------|
| SiO <sub>2</sub>               | 40.73  | 41.17  | 42.29  | 41.21  | 41.25  | 41.27  | 41.23  |
| TiO <sub>2</sub>               | 6.77   | 6.74   | 7.83   | 6.95   | 6.39   | 6.53   | 6.77   |
| Al <sub>2</sub> O <sub>3</sub> | 0.75   | 0.76   | 0.49   | 0.65   | 0.66   | 0.69   | 0.67   |
| FeO                            | 43.08  | 42.90  | 40.90  | 42.12  | 42.73  | 43.14  | 42.56  |
| MnO                            | 1.30   | 1.16   | 1.75   | 1.38   | 1.19   | 1.15   | 1.28   |
| CaO                            | 0.50   | 0.50   | 0.02   | 0.37   | 0.46   | 0.48   | 0.42   |
| Na <sub>2</sub> O              | 7.66   | 7.36   | 8.07   | 7.91   | 7.71   | 7.22   | 7.63   |
| Total                          | 100.79 | 100.59 | 101.33 | 100.59 | 100.39 | 100.48 | 100.56 |

Fe shown as FeO

- 1 S 68124. Mean of 2 analyses
- 2 S 68142. Mean of 3 analyses
- 3 S 68155. 1 analysis
- 4 S 68163. Mean of 11 analyses
- 5 S 68169. Mean of 3 analyses
- 6 S 68179. Mean of 7 analyses
- 7 Mean of 27 analyses.

Analyst R. R. Harding

#### Minor constituents

**Magnetite** Magnetite is rare in the microgranite and analyses of seven grains from five rocks show only minor variation in major element content (Table 5). An opaque grain in S 68155 differs from magnetite in the other thin sections in its exceptionally high contents of MnO (8.1% compared with a mean of 1.8%) and ZnO (7.1% compared with a mean of 1.4%).

**Table 5** Electron probe analyses of magnetite from the Ailsa Craig granite

|                                | 1     | 2     |
|--------------------------------|-------|-------|
| SiO <sub>2</sub>               | 1.23  | 0.66  |
| TiO <sub>2</sub>               | 11.48 | 24.95 |
| Al <sub>2</sub> O <sub>3</sub> | 0.27  | <0.2  |
| FeO                            | 74.69 | 53.52 |
| MnO                            | 1.79  | 8.13  |
| MgO                            | 0.11  | <0.2  |
| CaO                            | 0.08  | 0.15  |
| Na <sub>2</sub> O              | 0.67  | 0.80  |
| ZnO                            | 1.42  | 7.10  |
| Total                          | 91.74 | 95.31 |

Total iron given as FeO.

1 Mean of 7 analyses of magnetite from S 68124, S 68136, S 68142, S 68163 and S 68179.

2 Analysis of magnetite from S 68155.

Analyst R. R. Harding

**Fluorite** Fluorite has already been described as subhedral grains up to 0.5 mm across or more commonly as tiny inclusions in pyroxene or amphibole. Its greater abundance was noted in a sandstone xenolith (S 72698). Microprobe analyses indicate that the fluorite is fairly pure CaF<sub>2</sub> with 0.5 to 1.0% Y<sub>2</sub>O<sub>3</sub>, but no rare earth oxides above the detection limit of 0.4%.

**Pseudomorphs** Polygonal or subhedral crystals up to 0.5 by 0.4 mm occur rarely in several specimens (such as S 68131, 68138, 68149, 68156) (Plate 4e). They are formed of cryptocrystalline clay material with variable strings of iron oxide and 'leucoxene' dust. Six-sided crystals showing traces of a basal cleavage, prism and pyramid resemble replaced olivine; others may be after amphibole or pyroxene; pseudomorphs occur near drusy cavities. They may be mantled by arfvedsonite as in S 68138.

**Glauconite-celadonite** Electron microprobe analyses of pale green or brown fibrous minerals, which occur in a few interstitial patches scattered throughout the granite, indicate that two mica group minerals of slightly different composition are present. The first is very fine-grained granular or fibrous and its textures resemble those of serpentine pseudomorphs after olivine. Its composition is given in Table 6, column 1. The second mineral is platy or fibrous with a birefringence of 0.01–0.02, higher than that of the granular mineral. Its composition is given in Table 6, column 2 and by comparison it contains less Si, Al and Mg, and more Fe, Mn and K than the granular mineral. In S 68131 fibrous green and brown crystals occupy a small area 120 μm across between amphibole and feldspar. The green fibres are oriented at right angles to the amphibole edge and merge into turbid brown fibres at the centre of the patch. The green mineral is pleochroic from green to pale brown and shows variable birefringence up to 0.02. Similar interstitial patches, generally

**Table 6** Electron microprobe analyses\* of glauconite-celadonite from Ailsa Craig

|   | 1     | 2     | 3     | 4     |
|---|-------|-------|-------|-------|
| SiO <sub>2</sub>                              | 47.88 | 46.12 | 44.26 | 45.20 |
| Al <sub>2</sub> O <sub>3</sub>                | 5.45  | 4.75  | 9.11  | 5.17  |
| FeO   | 22.66 | 27.91 | 21.02 | 27.93 |
| MnO   | 0.19  | 0.67  | 0.20  | 0.40  |
| MgO   | 2.97  | 1.71  | 1.03  | 1.37  |
| CaO   | 0.24  | 0.22  | —     | —     |
| Na <sub>2</sub> O                             | 0.62  | 0.29  | —     | 0.26  |
| K <sub>2</sub> O                              | 7.54  | 9.00  | 8.25  | 8.60  |
| Cs <sub>2</sub> O                             | —     | 0.16  | —     | —     |
| ZrO <sub>2</sub>                              | 0.26  | —     | —     | —     |
| ZnO   | —     | 0.35  | —     | —     |
| <i>Total</i>                                  | 87.81 | 91.18 | 83.87 | 88.93 |
| <b>Atomic proportions based on 11 oxygens</b> |       |       |       |       |
| Si  | 3.70  | 3.57  | 3.63  | 3.57  |
| Al  | 0.30  | 0.43  | 0.37  | 0.43  |
| Al  | 0.20  | —     | 0.51  | 0.05  |
| Fe <sup>3+</sup>                              | 1.14  | 1.34  | 0.83  | 1.29  |
| Fe <sup>2+</sup>                              | 0.33  | 0.47  | 0.61  | 0.56  |
| Mn  | 0.01  | 0.04  | 0.01  | 0.03  |
| Mg  | 0.34  | 0.20  | 0.13  | 0.16  |
| Zn  | —     | 0.02  | —     | —     |
| Zr  | 0.01  | —     | —     | —     |
| Ca  | 0.02  | 0.02  | —     | —     |
| Na  | 0.09  | 0.04  | —     | 0.04  |
| K   | 0.74  | 0.89  | 0.86  | 0.87  |
| Cs  | —     | 0.01  | —     | —     |
| <i>Total cations</i>                          | 6.88  | 7.03  | 6.95  | 7.00  |
| Exchangeable cations                          | 0.85  | 0.96  | 0.86  | 0.91  |
| Fe <sup>3</sup> /Fe <sup>2</sup>              | 3.6   | 2.9   | 1.4   | 2.3   |

Total Fe given as FeO. Possible atomic proportions of Fe<sup>3+</sup> and Fe<sup>2+</sup> have been calculated on the basis of the glauconite formula.

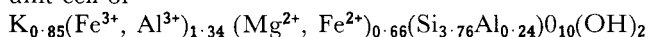
Oxides not detected (<0.2%) are marked with a dash.

- 1 Mean of 2 analyses of granular and fibrous glauconite, S 68169.
- 2 Mean of 2 analyses of platy glauconite, S 68169.
- 3 Mean of 3 analyses of fibrous and granular glauconite, S 68131.
- 4 Analysis of platy glauconite, S 29387.

*Analyst* R. R. Harding

\* From Harding (1983)

surrounded by feldspar, and numerous ill-defined flecks of the green mineral occur throughout the rock, and the mean of 3 analyses is given in column 3. In S 29387 a cluster of intergrown plates 1 mm across is completely enclosed by amphibole grains and an analysis is given in column 4. The equant grains show a good cleavage (bent in some of the larger grains) and strong pleochroism from yellow green to very pale green. There are irregular areas in some grains where the green merges into brown and the corresponding colour at right angles is very pale brown. All analyses given in Table 6 lie within the range for glauconites given by Buckley and others, (1978). The oxidation state of iron cannot be determined by microprobe analysis, and one way of calculating the atomic proportions is to assume that the minerals are glauconitic or celadonitic. Glauconite has an average half unit cell of



and celadonite approaches  $K(Fe^{3+}, Al^{3+})(Mg^{2+}, Fe^{2+})Si_4O_{10}(OH)_2$ .

Initial calculations on the Ailsa Craig mineral data assumed all the iron to be ferrous and the atomic proportions indicated that there was considerable substitution of Al and Si in the tetrahedral position. This suggested the minerals were glauconitic and subsequent calculations were made so that the iron was divided in such a way that octahedral (Fe<sup>3+</sup> + Al<sup>3+</sup>) totalled 1.34 in the half unit cell. With this assumption that the minerals are glauconitic the calculated atomic proportions are given in Table 6.

In order to determine other trace minerals that might be present, bromoform (specific gravity 2.9) separations were made of five samples of the microgranite, further separated electromagnetically at 0.8 and 1.0 amps, and splits examined optically by immersion in calibrated refractive index liquids. The bulk of the heavies (ferromagnesian minerals) were separated off in the magnetic at 0.8 amps fractions.

*Zircon*: colourless, clear euhedral prisms and pyramids averaging 0.2 × 0.1 mm; relatively common in the non-magnetic fractions.

*Monazite*: Pale yellow, glassy (001) tablets and stumpy prisms showing emerald-green under the mercury vapour spectrum (Murata and Bastron, 1956).

*Rutile*: dark brown to yellow prisms, pyramids and twinned crystals, relatively conspicuous in samples S 68168 (granite screen in a multiple dyke complex) and in S 68179.

*Apatite*: elongated colourless to pale yellow prisms up to 0.3 × 0.06 mm.

*Brookite*: pale yellow glassy crystal fragments up to 0.2 mm; relatively common in S 68168, and probably accounts, with rutile for most of the TiO<sub>2</sub> in the whole-rock analysis. Identification was confirmed by X-ray diffraction photograph by Mr B. R. Young (X8567).

*Pyrite*: polyframboidal to coarser fragments; relatively conspicuous in S 68169. Mackie (1928) recorded olivine and garnet in addition to the above minerals, though these may probably have stemmed from xenoliths of country rock.

*Amorphous mineral* Patches of dark brown material occur at the cores of amphibole or aenigmatite grains, or in the interstices between quartz and feldspar in a poikilitic habit similar to that shown by the margins of amphiboles and aenigmatites. Microprobe analyses indicate that grains of anatase or rutile, sphene and aenigmatite are commonly present in the dark brown masses so the variation in composition from point to point probably depends on the different proportions of a number of components.

*Gypsum* Suspected specimens of 'guano' found by Dr A. T. J. Dollar at the foot of Main Craigs (or Goose Craigs), and also in the present survey along the west cliffs, proved on X-ray diffraction analysis (X 8564) by Mr B. R. Young to be gypsum. This occurs as off-white botryoidal masses up to 1 cm in thickness.

#### *Modal analyses*

Broad groups of the major minerals were quantified by means of the computerised image analyser (Dearnley, 1979), and the results are given in Table 7.

**Table 7** Modal analyses of microgranites by computerised image analysis

| Sample Ref. No. | Lithology                | Brief locality                       | Volume per cent                |                 |        |
|-----------------|--------------------------|--------------------------------------|--------------------------------|-----------------|--------|
|                 |                          |                                      | Total ferro-magnesian minerals | Alkali feldspar | Quartz |
| S 68124         | Leucomicrogranite        | Northwest cliff base                 | 0.01                           | 84.44           | 15.55  |
| S 68126         | Leucomicrogranite        | Northwest cliff base                 | 0.69                           | 86.89           | 12.42  |
| S 68129         | Leucomicrogranite        | Northwest cliff base                 | 0.05                           | 86.62           | 13.33  |
| S 68150         | Leucomicrogranite        | Northeast (curling stone quarry)     | 0.17                           | 73.96           | 25.88  |
| S 68169         | Leucomicrogranite        | Upper Craig                          | 0.44                           | 84.83           | 14.23  |
| S 68179         | Leucomicrogranite        | Near top of Craig                    | 0.08                           | 59.33           | 40.59  |
|                 |                          | <i>Mean of leucomicrogranites</i>    | 0.24                           | 79.35           | 20.41  |
| S 68121         | Spotted microgranite     | West cliff base                      | 0.07                           | 82.72           | 17.20  |
| S 68131         | Spotted microgranite     | North cliff base                     | 0.03                           | 79.84           | 20.12  |
| S 68142         | Spotted microgranite     | West cliff base                      | 0.35                           | 78.42           | 21.22  |
| S 68136         | Spotted microgranite     | East cliff base                      | 0.13                           | 77.31           | 22.56  |
| S 68155         | Spotted microgranite     | Northeast cliff base                 | 0.14                           | 62.45           | 37.41  |
| S 68163         | Hematitised microgranite | Southeast cliff base                 | 0.06                           | 66.15           | 33.78  |
| S 68168         | Spotted microgranite     | South cliff base                     | 0.30                           | 84.44           | 15.25  |
|                 |                          | <i>Mean of spotted microgranites</i> | 0.16                           | 75.90           | 23.94  |

Analyst R. Dearnley

## CHEMISTRY

### Major elements

Six samples of microgranite collected peripherally around the island were fully analysed by direct reading emission spectrometry and wet chemical methods. The results are listed in Table 8, where the samples are grouped on a basis of increasing Colour Index (CI). The means of the six samples are compared with the analysis by Rault (*in Lacroix, 1923*), and with two analyses by Dr A. T. J.

Dollar (unpublished). There is little significant variation between the samples individually, confirming the overall chemical homogeneity of the microgranite. There is a slight increase in CaO with CI, reflecting mainly concomitant increase in aegirine and (to a less extent) the arfvedsonite. However, FeO, which is contained mainly in those two minerals, does not increase with CI. The marked macroscopic differences, therefore, emphasised by the size and concentration of black druses mainly filled with quartz and ferromagnesian minerals, are not reflected

**Table 8** Whole rock chemical analyses of microgranites

| Colour Index   | 5-10%   |         | 10-15%  |         | 15-25%  |         | Mean of 6 analyses | Range | A                      | B      | C     |
|--|---------|---------|---------|---------|---------|---------|--------------------|-------|------------------------|--------|-------|
|  | S 68150 | S 68179 | S 68163 | S 68168 | S 68169 | S 68142 |                    |       |                        |        |       |
| SiO <sub>2</sub>   | 71.9    | 70.6    | 70.9    | 70.8    | 70.9    | 70.6    | 70.95              | 1.30  | 71.56                  | 70.95  | 71.62 |
| Al <sub>2</sub> O <sub>3</sub>   | 14.5    | 14.9    | 15.0    | 14.6    | 14.8    | 14.9    | 14.8               | 0.50  | 14.02                  | 14.91  | 8.13  |
| Fe <sub>2</sub> O <sub>3</sub>   | 1.55    | 1.51    | 1.66    | 1.61    | 1.54    | 1.54    | 1.57               | 0.15  | 1.26                   | 0.95   | 6.27  |
| FeO  | 0.91    | 0.96    | 0.85    | 0.87    | 0.95    | 0.94    | 0.91               | 0.10  | 1.46                   | 1.31   | 1.84  |
| MgO  | 0.11    | 0.12    | 0.12    | 0.48    | 0.11    | 0.10    | 0.17               | 0.38  | 0.21                   | 0.22   | 0.04  |
| CaO  | 0.30    | 0.32    | 0.36    | 0.36    | 0.38    | 0.41    | 0.36               | 0.11  | 0.42                   | 0.52   | 0.23  |
| Na <sub>2</sub> O  | 6.40    | 6.41    | 6.45    | 6.04    | 6.47    | 6.50    | 6.38               | 0.46  | 6.46                   | 6.48   | 4.69  |
| K <sub>2</sub> O   | 4.08    | 4.29    | 4.32    | 4.70    | 4.30    | 4.25    | 4.32               | 0.62  | 3.97                   | 4.17   | 5.31  |
| TiO <sub>2</sub>   | 0.05    | 0.06    | 0.06    | 0.06    | 0.06    | 0.06    | 0.06               | 0.01  | 0.28                   | 0.09   | 0.19  |
| P <sub>2</sub> O <sub>5</sub>  | 0.02    | 0.02    | 0.02    | 0.03    | 0.03    | 0.06    | 0.04               | 0.04  | tr                     | nil    | 0.36  |
| MnO  | 0.05    | 0.06    | 0.06    | 0.07    | 0.06    | 0.06    | 0.06               | 0.02  | —                      | tr     | 0.10  |
| F  | 0.18    | 0.16    | 0.20    | 0.15    | 0.18    | 0.21    | 0.18               | 0.06  | —                      | n.d.   | —     |
| Loss on ignition corrected for volatiles and Fe <sup>2+</sup> , Fe <sup>3+</sup> | 0.27    | 0.24    | 0.24    | 0.48    | 0.28    | 0.24    | 0.29               | 0.24  | H <sub>2</sub> O* 0.43 | 0.18   | 0.36  |
| H <sub>2</sub> O <sup>-</sup>  | 0.19    | 0.22    | 0.24    | 0.42    | 0.28    | 0.32    | 0.28               | 0.13  | 0.08                   | 0.28   | 0.23  |
|  | 100.51  | 99.87   | 100.48  | 100.67  | 100.34  | 100.19  |                    |       |                        |        |       |
| Less O, F  | 0.08    | 0.06    | 0.08    | 0.06    | 0.08    | 0.08    | —                  | —     | —                      | —      | —     |
| Total  | 100.43  | 99.81   | 100.40  | 100.61  | 100.26  | 100.11  | 100.37             | —     | 100.15                 | 100.06 | 99.37 |

Analysts A. E. Davis and M. Dawkins, Analytical Chemistry Unit, BGS

Samples (S) Ailsa Craig; this paper

A Riebeckite-microgranite, Ailsa Craig. Analyst Rault in Lacroix (1923)

B Mean of two analyses (1) from 'Blue Hone' New Quarry, NE coast, Ailsa Craig (2) 'Common Rock' (medium grade) Trammins, Ailsa Craig Analyst A. T. J. Dollar, unpublished.

C Aegirine-acmite-riebeckite-granite, Rockall Island. Analysts J. M. Murphy and G. A. Sergeant (*in Hawkes and others, 1975*).

significantly in the whole-rock chemistries. With the exception of Fe<sub>2</sub>O<sub>3</sub> and FeO, the means of the present analyses are similar to those quoted by Rault *in* Lacroix (1923), and by Dr A. T. J. Dollar (unpublished) (Table 8). The aegirine-granite of Rockall Island differs from both in having lower Al<sub>2</sub>O<sub>3</sub> and much higher Fe<sub>2</sub>O<sub>3</sub>, a little higher FeO and K<sub>2</sub>O; these account for the greater abundance in the Rockall granite of aegirine and riebeckite (Sabine, 1960).

The Holy Island (Arran) trachyte consists (S 24461) of sanidine microphenocrysts and ophitic or sponge-like plates of riebeckite in a fluxioned groundmass of sanidine, riebeckite, aegirine-augite, iron oxides, and a little (3 to 5%) free quartz which occurs interstitially to the feldspars. With the occurrence of sodic amphibole and pyroxene, there is some relation with the Ailsa Craig microgranite, but the Holy Island trachyte has lower SiO<sub>2</sub>, MgO, Na<sub>2</sub>O, and higher K<sub>2</sub>O and P<sub>2</sub>O<sub>5</sub>.

The CIPW norms are listed in Table 9, together with Alpaicity and Differentiation indexes. In general terms the norms correspond broadly with the modes (Table 7) especially in mean feldspar contents, though allowance must be made for sampling (thin sections *vs* crushed whole rocks). The modes indicate an enrichment in quartz in the most leucocratic samples, from the old curling stone quarry and from the Upper Craig; this enrichment is at the expense mainly of feldspar and is evidently late-stage permeation. To this extent, therefore, this lithology appears to represent the latest phase in the granite crystallisation sequence, and the finer grain suggests proximity to country rock contacts at the north-east face and the roof to the intrusion.

#### Trace element geochemistry

Three samples (leucomicrogranite, drusy microgranites) were analysed for trace elements by spark-source mass spectrometry. This is a semi-quantitative survey method and while the data can be expressed only as a probable range covering one order of magnitude, nevertheless it is particularly useful since it covers most elements in the Periodic Table except those which are subject to interferences. Where interference is known or suspected then the range is reported as 'less than' maximum concentration. The results are listed in Table 11. Additional trace elements – Nb, Y, Zr, Sr and Pb – were analysed by XRF, rare earth elements (REE) – La, Ce, Nd, Sm, Eu, Tb, Ho, Yb and Lu – by neutron activation (Table 10). The rare earths are normalised to standard chondrite (using the values of Haskin, 1979; Haskin and others, 1968) in Figure 4, and show enrichment in L-REEs (relative to H-REE) and a pronounced negative Eu anomaly due to extraction, during fractionation, by alkali feldspar. There is little significant difference between the two microgranites after allowing for errors based on counting statistics – 10% (La), 5% (Ce), 10% (Nd), 2% (Sm), 5% (Eu), 10% (Tb) and 3% (Ho, Yb, La). The light-to-heavy REE ratio La<sub>N</sub>:Yb<sub>N</sub> = 2.89 (drusy microgranite) and 1.96 (leucomicrogranite), the latter ratio according with that for the sample quoted by Meighan (1979), and with the negative Eu-anomaly indicates a very fractionated alkalic granitic residuum; the La:Nb ratio is very low compared with other Tertiary acid intrusives of Scotland. Of the other trace elements, Zr is relatively high (compared with the last-named except the Rockall granite which is enriched in Zr), and is accounted

**Table 9** Norms of microgranites, Ailsa Craig

| Sample No.            | Leucomicrogranites |         |         | Drusy microgranites |         |         | Mean  |
|-----------------------|--------------------|---------|---------|---------------------|---------|---------|-------|
|                       | S 68150            | S 68179 | S 68163 | S 68168             | S 68169 | S 68142 |       |
| Q                     | 19.39              | 17.08   | 16.96   | 17.39               | 17.18   | 16.87   | 17.48 |
| Ab                    | 51.86              | 53.08   | 53.13   | 49.06               | 52.32   | 53.20   | 52.11 |
| Or                    | 24.08              | 25.48   | 25.51   | 27.81               | 25.44   | 25.19   | 25.59 |
| Ac                    | 1.96               | 1.26    | 1.24    | 1.87                | 2.21    | 1.73    | 1.71  |
| Di                    | 0.03               | 0.22    | 0.15    | 0.38                | 0.29    | 0.08    | 0.19  |
| Hy                    | 0.26               | 0.20    | 0.23    | 1.02                | 0.14    | 0.21    | 0.34  |
| Hm                    | 1.88               | 2.16    | 2.17    | 1.94                | 1.84    | 1.99    | 1.99  |
| Ap                    | 0.05               | 0.05    | 0.05    | 0.07                | 0.07    | 0.14    | 0.07  |
| Ru                    | 0.05               | 0.06    | 0.06    | 0.06                | 0.06    | 0.06    | 0.06  |
| Fl                    | 0.37               | 0.33    | 0.41    | 0.31                | 0.37    | 0.43    | 0.37  |
| <i>Total</i>          | 99.92              | 99.92   | 99.92   | 99.92               | 99.92   | 99.92   | 99.91 |
| Alpaicity             | 1.03               | 1.02    | 1.02    | 1.03                | 1.03    | 1.03    | 1.03  |
| Differentiation Index | 95.32              | 95.64   | 95.61   | 94.26               | 94.94   | 95.27   | 95.17 |

**Table 10** Neutron activation analyses of microgranites for rare-earth elements

| S     | Atomic weight                | La<br>57 | Ce<br>58 | Pr<br>59 | Nd<br>60 | Sm<br>62 | Eu<br>63 | Gd<br>64 | Tb<br>65 | Dy<br>66 | Ho<br>67 | Er<br>68 | Yb<br>70 | Lu<br>71 |
|-------|------------------------------|----------|----------|----------|----------|----------|----------|----------|----------|----------|----------|----------|----------|----------|
| 68150 | Leucomicrogranite            | 47.7     | 154      |          | 91.8     | 25.5     | 1.78     |          | 5.72     |          | 12.7     |          | 17.4     | 2.52     |
| 68142 | Spotted (drusy) microgranite | 62.3     | 187      |          | 95.8     | 25.4     | 1.99     |          | 4.92     |          | 7.6      |          | 15.0     | 2.15     |
| —     | Microgranite (Meighan, 1979) | 44.2     | 126      | 19.5     | 81.8     | 19.3     | 1.5      | 21.3     | 3.2      | 20.5     | 3.81     | 14.2     | 15.0     | 2.2      |

Figures are given in parts per million

*Analyst* Dr Susan Parry, University of London Reactor Centre, Silwood Park, Ascot, Berkshire

**Table 11** Spark source mass spectrometry analyses

| Elements     | Microgranites |          |        | Basalt   |                 |
|--------------|---------------|----------|--------|----------|-----------------|
|              | 1             | 2        | 3      | 4        |                 |
| <b>IA</b>    | Rb            | 60–600   | 20–200 | 60–600   | 0.6             |
|              | Cs            | <3       | <3     | <1       | <1              |
|              | Mg            | 20–200   | 20–200 | 20–200   | (major element) |
|              | Ca            | 300–3000 | 0.1–1% | 100–1000 | (major element) |
| <b>IIA</b>   | Sr            | <3       | <3     | <3       | 2–20            |
|              | Ba            | 6–60     | 20–200 | 6–60     | 60–600          |
| <b>IIIB</b>  | Y             | 20–250   | 20–250 | 10–100   | 3–30            |
|              | La            | 3–30     | 3–30   | 3–30     | 1–10            |
| <b>IVB</b>   | Zr            | 100–1500 | 60–600 | 60–600   | 10–150          |
|              | Hf            | <6       | <6     | 2–20     | <2              |
| <b>VB</b>    | Nb            | 10–100   | 20–250 | 10–100   | 1–10            |
|              | Ta            | <2       | <2     | <2       | 0.6             |
| <b>VIB</b>   | W             | 20–200   | 6–60   | 6–60     | 20–200          |
| <b>VII B</b> | Mn            | 100–1500 | 60–600 | 100–1500 | <0.1            |
| <b>IB</b>    | Cu            | 1–10     | 1–10   | 1–10     | 30–300          |
|              | Zn            | 60–600   | 60–600 | 20–200   | 20–200          |
| <b>IIB</b>   | Cd            | <1       | <1     | <1       | <1              |
|              | Hg            | <6       | <2     | <2       | <6              |
| <b>IIIA</b>  | Ga            | 30–300   | 30–300 | 10–100   | 10–100          |
|              | Tl            | <1       | <1     | <1       | 0.01–0.1        |
| <b>IVA</b>   | Ge            | <6       | <6     | <2       | <2              |
|              | Sn            | 1–15     | 1–10   | 1–15     | <2              |
|              | Pb            | 10–100   | 3–30   | 10–100   | <3              |
| <b>VA</b>    | As            | <2       | <2     | <0.6     | <0.6            |
| <b>VIA</b>   | S             | 6–60     | 6–60   | 6–60     | 60–600          |
|              | Se            | <3       | <10    | <10      | <10             |
| <b>VIIA</b>  | Cl            | 30–300   | 10–100 | 10–150   | 30–300          |
|              | F             | 60–600   | 60–600 | 20–200   | 6–60            |
|              | Br            | <2       | <2     | <2       | <6              |
| <b>IIIB</b>  | Ce            | 10–150   | 10–150 | 10–150   | 6–60            |
|              | Pr            | 3–30     | 3–30   | 1–10     | 1–10            |
|              | Nd            | 20–250   | 6–60   | 10–100   | 6–60            |
|              | Sm            | 1–15     | 1–15   | 2–20     | 1–15            |
|              | Eu            | <3       | <3     | <3       | 1–10            |
|              | Gd            | 2–20     | 1–15   | 2–20     | 2–20            |
|              | Tb            | 0.3–3    | 0.3–3  | 0.6–6    | 0.1–2           |
|              | Dy            | 2–20     | 2–20   | 2–20     | 2–20            |
|              | Ho            | 0.6–6    | 0.3–3  | 0.6–6    | 0.1–2           |
|              | Er            | 1–15     | 1–10   | 1–15     | <3              |
|              | Tm            | <2       | <2     | <2       | <2              |
|              | Yb            | <6       | <6     | <6       | <6              |
|              | Lu            | <2       | 0.1–2  | <2       | 0.6             |
|              | Th            | 0.6–6    | <2     | 0.6–6    |                 |
|              | U             | <2       | <0.6   | <2       |                 |

*Samples*

- 1 S 68150 Aegirine-arfvedsonite-microgranite, Ailsa Craig (Leucomicrogranite)
- 2 S 68169 Aegirine-arfvedsonite-microgranite, Ailsa Craig (Drusy spotted microgranite)
- 3 S 68179 Aegirine-arfvedsonite-microgranite, Ailsa Craig (Drusy spotted microgranite)
- 4 S 68151 Tholeiite dyke, Ailsa Craig

Elements not shown are either below the limits of detection or not sought because of interference

Analysed by the Analytical Research and Development Unit, AERE, Harwell.

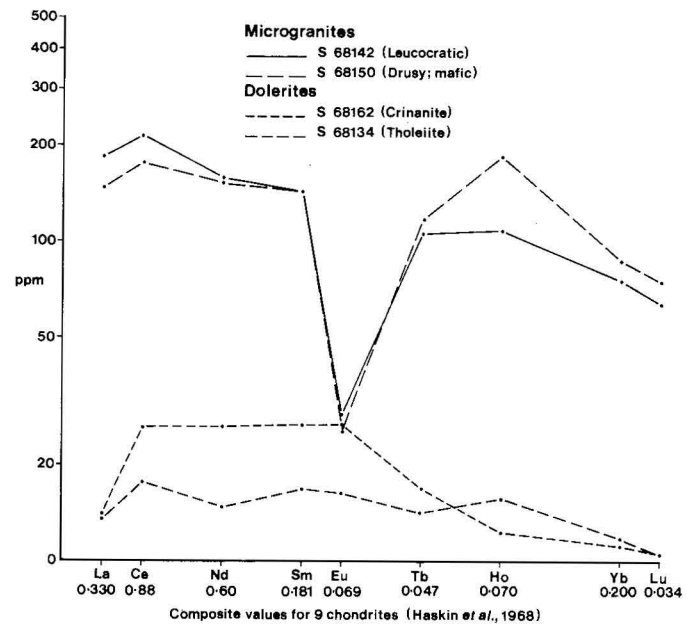


**Figure 4** Normalised rare earth plots for microgranites and basic dykes.

for by accessory zircon described above. Zinc is also relatively abundant (60 to 600 ppm); the world-wide average for low-calcium granites is 39 ppm (Turekian and Wedepohl, 1961). Data for the UK Tertiary granites are sparse except for the Rockall aegirine/acmite-riebeckite-granite which has a similar Zn content. No Zn-mineral *per se* has yet been identified from Ailsa Craig, although it is a minor element in some of the amphiboles, magnetites and glauconites.

Because gold had been reported from the Ailsa microgranite (Heddle, 1897) analyses of five samples for both Au and Ag were made by neutron activation analysis (analyst Dr Susan Parry). All five contained no detectable Au and Ag (<0.02 ppm and <2 ppm respectively; errors 10% and 30% respectively). Therefore attempts were made by Dr J. D. Bignell\* to concentrate any gold and silver present by froth flotation (details in Appendix 1). Two concentrates ex- S 68131 and 68136 (the scavenger and rougher concentrates) were then analysed and found by Dr Parry to contain 0.21 ppm Au, 3.9 ppm Ag; and 0.65 ppm Au and 9.7 ppm Ag respectively. Thus gold and silver apparently exist in the Ailsa microgranite but the levels are extremely low and no discrete minerals have been recognised. Minute inclusions in vughy quartz appear to be metallic, but are probably pyritic. Nevertheless the fact that flotation markedly upgrades the Au and Ag suggests the presence in the microgranite of discrete specks of these minerals, albeit at very low levels.

Through the courtesy of the Curator, Mr J. Hunter, Dick Institute, Kilmarnock, the original thin sections were made available from which James Blackwood, an amateur scientist, had ostensibly detected the gold specks noted in Heddle (1897). Careful re-examination of these slides showed no gold, though the minute metallic inclusions in drusy quartz, referred to above, which are probably pyrite, may have been mistaken for the precious metal.

In summary, the microgranite is chemically homogeneous over much of its accessible outcrop despite the superficial macroscopic lithological differences. It differs markedly from the Rockall aegirine/acmite-riebeckite-granite in the latter's much lower Al<sub>2</sub>O<sub>3</sub> and

\* Warren Spring Laboratory, Department of Industry, Gunnels Wood Road, Stevenage, Hertfordshire.

**Table 12** Rb-Sr analyses of the arfvedsonite-aeirine-microgranite, Ailsa Craig

| XRF results |        |        |              | Isotope dilution results |        |                                    |                                    |
|-------------|--------|--------|--------------|--------------------------|--------|------------------------------------|------------------------------------|
| Sample no.  | Rb ppm | Sr ppm | Rb/Sr atomic | Rb ppm                   | Sr ppm | <sup>87</sup> Rb/ <sup>86</sup> Sr | <sup>87</sup> Sr/ <sup>86</sup> Sr |
| S 68126     | 164    | 3.5    | 47.3 ± 5%    | 174.3                    | 3.81   | 133.74                             | 0.81916 ± 0.03%                    |
| S 68129     | 146    | 3.0    | 48.6 ± 5%    | —                        | —      | —                                  | —                                  |
| S 68131     | 145    | 11.3   | 13.2 ± 2%    | —                        | —      | —                                  | —                                  |
| S 68136     | 143    | 2.0    | 73.4 ± 10%   | —                        | —      | —                                  | —                                  |
| S 68142     | 139    | 2.5    | 57.7 ± 8%    | 152.0                    | 2.77   | 160.63                             | 0.84426 ± 0.02%                    |
| S 68150     | 152    | 1.5    | 104.2 ± 12%  | 164.5                    | 1.80   | 270.80                             | 0.94078 ± 0.04%                    |
| S 68155     | 142    | 1.3    | 108.7 ± 15%  | 153.4                    | 1.58   | 288.38                             | 0.95346 ± 0.008%                   |
| S 68163     | 140    | 1.8    | 79.1 ± 10%   | 150.3                    | 2.07   | 213.77                             | 0.89001 ± 0.03%                    |
| S 68168     | 156    | 7.0    | 22.8 ± 3%    | 168.6                    | 7.64   | 64.20                              | 0.75882 ± 0.009%                   |
| S 68169     | 144    | 2.2    | 66.6 ± 8%    | 154.8                    | 2.47   | 184.13                             | 0.86395 ± 0.03%                    |
| S 68179     | 143    | 1.3    | 114.0 ± 15%  | 151.1                    | 1.67   | 208.33                             | 0.93557 ± 0.04%                    |

Initial ratio 0.7028 ± 0.0009

Age 62 ± 0 Ma

Analyst Mrs Maureen Brook

higher total Fe, lower Na<sub>2</sub>O but higher K<sub>2</sub>O. Accordingly the Ailsa Craig microgranite does not lie on any of the trends in the plot of Al/Fe against Si/(Na + K) (Hawkes and others, 1975), and on this basis at least does not appear to have a direct genetic relation to the Rockall granite.

#### Isotopic age determination

Although the Tertiary age of the Ailsa Craig microgranite has long been known, there has been no modern accurate absolute age determination. The extensive sampling of the intrusion over much of its accessible outcrop provides, the best possible sample range for Rb/Sr isotopic dating. Initial analyses by XRF on 11 samples (Table 12) gave very low levels of Sr and Rb/Sr ratios precise only to about ± 5 to 15%. Accordingly eight samples showing the widest range of Rb/Sr values were selected for further analysis by the more precise isotope dilution method. These results are shown in Table 12, data being regressed to the method of York (1969). The regressed points are shown in Figure 5 and yield an isochron giving an age of 61.5 ± 0.5 Ma which we consider to be the age of intrusion. The initial <sup>87</sup>Sr/<sup>86</sup>Sr ratio of 0.7028 ± 0.0009 is extremely low for an acid igneous rock, and falls within the range of the lowest values for alkali basalts, dolerites and mugearites from other Tertiary intrusive centres in the

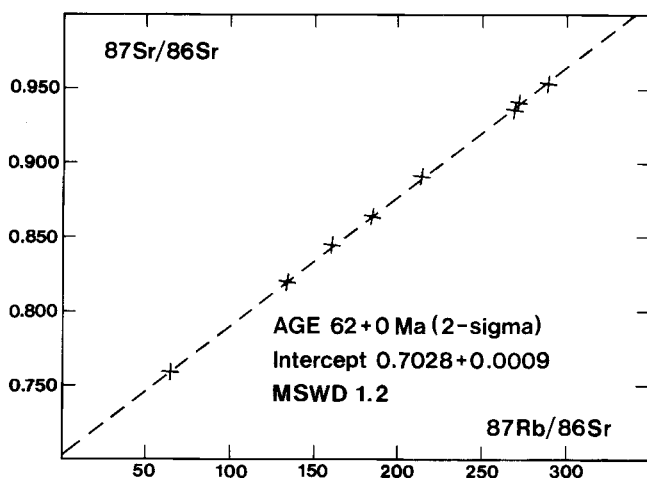


**Figure 5** Diagram showing Rb and Sr ratios and an isochron for the Ailsa Craig microgranite.

north-west Scotland Tertiary province. Moreover the age of 61.5 ± 0.5 Ma is the oldest recorded of any acid intrusion in this province, including the Rockall aegirine-riebeckite-granite (52 Ma), (Hawkes and others, 1975) and the granophyres of St Kilda (Brook *in* Harding and others, 1984).

## BASIC DYKES

### GENERAL DESCRIPTION

One of the most striking features of the British Tertiary igneous province is the general NW-SE trend of the dyke swarms. Within this general pattern, the Arran swarm is notable with its marked concentration of NNW-SSE dykes, and the degree of dilation. This trend has been related (Evans, 1925) to the extensive 'deep' stretching north-west from the Bay of Biscay into the Atlantic, and, significantly, to crustal stretching towards that 'deep' and normal to the NW-SE trend of the dyke-swarms. Though predating modern concepts of the opening of the North Atlantic and plate movements by some 40 years, this idea clearly anticipated these concepts and their foundation on geomagnetic and other evidence of crustal movements. The Arran dyke swarms are mentioned briefly here because of their geographical proximity to Ailsa Craig, which lies only 20 km to the south. Dagley and others (1978), in a palaeomagnetic study of these swarms, found normal polarities (polarity does not correlate with petrography) with the rocks being formed during an R-N-R sequence of polarities; the isotopic age of 58 Ma for the Northern Arran granite was used and the intrusive period of the dykes estimated to be 0.5 to 3.4 Ma if three polarity periods were involved and 3.4 to 4.4 Ma if four were involved. The individual Tertiary dykes of Ailsa Craig strike mainly N-S to NNE-SSW, with subordinate NE-SW and minor NNW-SSE orientations. The most prominent trends shown by the erosional features of the dykes lie almost N-S and NE-SW. It is difficult to follow inland the many dykes seen around the cliff perimeter, partly because of extensive patches of scree, and also because of the inaccessibility of much of the upper slopes of the Craig. While most of the coastal exposures give the impression of separate dykes, some may coalesce while others bifurcate. Thicknesses range from 0.1 to 4.7 m, and in composite dykes with granite screens

to nearly 6.0 m, as exposed in the pathway from sea-level up to the Castle. The average thickness excluding screens is about 1.4 m, compared with 3.6 m for the Arran dykes (Tyrrell, 1928). Most of the dykes are vertical or subvertical with only very localised flexuring or coalescence (for example at Macanall's Cave), bifurcation or sidestepping. As noted above, the microgranite, which is intruded by the dyke swarm, is itself cut by subvertical joints, with distribution modes at NW, NNW and NE, and so the emplacement of the dykes has to a large extent been controlled by these joint-patterns. However, no low-dipping basalt sheets occur along the quaquaversal 'floor' jointing of the microgranite. Forty-three dyke exposures were mapped during the survey, though no single dyke could be traced as a continual outcrop across the Craig. The slacks are firm evidence of underlying dykes, now deeply weathered and concealed by scree, soil or peat and the likely continuity of the dyke outcrops mapped around the coast is evident from the map and the inclined aerial photograph (Plate 1). With the exception of the projected connections of the dykes exposed near Macanall's Cave with those of 'Slunk' (NW coast) and of those from Rotten Nick and East Trammins which join Garra Loch and strike NNW to Swine Cave on the north coast, it is not possible to project and connect the individual outcrops around the coasts. Dollar, however, connected the thick dyke complex exposed in the path up to the castle with the first dyke exposed north of the jetty, at Swine Holes. The steepness of the ground did not allow a traverse along this dyke. The depression, in which thick peat has accumulated with seasonal lochans at Garra Loch, has arisen through deep erosion of the meeting of several dykes hereabouts. Comparing the widths of the slacks with the thicknesses of their respective dykes as exposed around the coasts, shows that the former are in general much thicker due to lateral widening of the eroded gully, but whether glacial excavation contributed to this widening is uncertain.

#### PETROGRAPHY

The thicker dykes are complex, with several distinct subparallel units which usually comprise basalt against the contact walls, dolerite interiors, and, in places, screens of microgranite. The basaltic marginal zones commonly show spheroidal weathering and are more friable due to weathering than doleritic interiors. Specimens were collected where possible from 43 outcrops of dykes (numbered in Roman numerals) and the following petrographical account is based on thin sections of these specimens together with an examination of 53 thin sections of dyke specimens collected by Dollar. Wherever possible, the collecting sites of the latter specimens have been related to those of the present survey and the two sets of observations thus combined in this account. Constraints in this correlation have been imposed by the smallness of scale of the 1:10 560 base map used by Dollar and its generalised features for the detail required for the many exposures. The modern 1:10 000 base map is similarly too small in scale to depict the dykes with sufficient accuracy.

The rocks, where fresh, are medium dark grey (N4) to dark grey (N3) and range from basalts with mean grain size of less than 0.1 mm to coarse dolerites with mean crystallinity of about 1 mm. Contacts of basaltic units are generally very weathered. Joints are well developed in the dykes and tend to lie normal to the contacts with microgranite, giving rise on denudation to a step-like structure.

Petrographically the dyke rocks are basaltic (mainly olivine-bearing), olivine-dolerites, olivine-poor dolerites and crinanitic olivine-dolerites and these are depicted on the map. There are all gradations between these three main varieties of dolerite and there is neither obvious relation between petrography and strike, nor any apparent constancy of composition along the dykes, though paucity of exposure over the Craig itself precludes any firm interpretation of the available exposures. On the contrary, all these dolerite varieties may occur in the same dyke complex, as in the area of Macanall's Cave – Stranry Point. The commonest variety is olivine-dolerite; olivine-poor dolerites occur (apart from the previously mentioned locality) near Craignaon (dykes XXXVII, XXXVIII), Swine Cave (XXI), below Slunk (XIII) and in the major dyke complex (XXXIX), exposed in the footpath to the Castle.

Crinanitic dykes (dolerites containing olivine and accessory analcime usually with zeolites), occur near Rotten Nick (XXVIII), Dalton's Cove (XXXV), below Slunk (XIV) and near Macanall's Cave (XXII). Volumetrically, olivine-dolerites predominate, if the available exposures are a true representation of the entire dyke-swarm. While the three main types are discussed in detail below, they are evidently comagmatic, the principal magma being olivine-dolerite and the olivine-poor and olivine-rich crinanitic types being local derivatives. Texturally, those specimens containing a glassy (now altered) mesostasis can be classified with tholeiites, but in view of the imprecise definitions of 'tholeiite' and its use as a rock series or trend, the term is not used here. The textural term is denoted as 'tholeiitic'. On the alkali-silica diagram of the IUGS classification the present dykes all plot in the Basaltic Rock field.

#### *Olivine-dolerites; olivine-basalts*

Texturally, these range from ophitic to subophitic, and feldspar- or olivine-microphyric to aphyric (basalts) (Plate 4h). In the phytic varieties, microphenocrysts are generally less than 2 mm in length but feldspars may attain 4.3 mm. These have cores ranging between  $An_{68}$  and  $An_{84}$  (labradorite to bytownite) zoned out to labradorite. Clinopyroxene varies in thin section from pale brown (such as S 68139) ('biscuit'), yellow-brown, purple-brown to deep purple or plum-coloured (S 68167). It forms ophitic or subophitic intergrowths with the plagioclase or in places is skeletal in optically continuous growths (S 68120), or fasciculate clusters (S 68167). Optically the augite has 2V (+) near 60°. Olivine where fresh is colourless but both phenocrysts and groundmass olivine are commonly altered to 'bowlingite', chlorite, smectite, serpentine minerals or 'viridite' (as in S 68133). Other accessories include opaque iron/titanium oxide forming plates, skeletal crystals or grains, and sporadic very minor to trace crystals of brown spinel (S 68135, 68137, 68158) associated with magnetite. Mesostasis varies from evidently altered glassy residuum (tholeiitic texture) to microcrystalline chlorite, radially fibrous zeolite and smectite patches. Some glassy material occupies original steam holes associated with hematite (S 68164, 68192). Radially fibrous zeolite may also occupy amygdaloids with smectite, carbonate or chlorite. Chlorophaeite was tentatively identified in S 68158. Visual estimates of approximate mineral abundance indicate plagioclase ranging between 40–60%, clinopyroxene 15–45%, olivine (and pseudomorphs) 5–25%, the remainder comprising opaque ore and secondary clay minerals.

*Olivine-poor dolerites*

These differ from the above only in containing less than about 5% by volume of olivine or its pseudomorphs. Olivine-poor rocks include feldspar-microphyric basalt (such as S 68157) and ophitic or subophitic dolerites (S 68161) with bytownite to labradorite microphenocrysts up to 2 mm long in a matrix of labradorite to bytownite and pale brown to purple-brown augite, opaque iron oxide and variable mesostasis or chlorite/smectite. In S 68157, (?) chlorophaeite occupies steam holes, with possible altered glassy mesostasis. Visual estimates give feldspar 45–60% by volume; augite 20–45%, 5–12% opaque ore, very minor olivine in places and the remainder mesostasis/amygdales.

*Crinanitic dolerites*

Crinanite is essentially analcime-dolerite (less analcimitic and zeolitic than teschenite, with olivine content about 22% by volume). The crinanitic dolerites of Ailsa contain up to 5% intersertal analcime with radially fibrous zeolite occupying steam cavities; augite is in excess of olivine with between 22–40% of the former and between 8–20% of the latter, plagioclase ranging between 35–45%. Thus there is a gradation between olivine-dolerite and analcime-olivine-dolerite tending towards crinanite. Examples of the nearest approach to crinanite (S 68123, 68170), are olivine-phyric with ophitic groundmass consisting of microcrystalline calcic plagioclase (0.5 mm laths) (35–45%), pale purple augite (22–30%), olivine

**Table 13** Microprobe analyses of olivine crystals from tholeiitic and crinanitic dykes, Ailsa Craig

|                  | Tholeiitic dolerites              |        |         |       | Crinanitic dolerites              |        |         |        |
|------------------|-----------------------------------|--------|---------|-------|-----------------------------------|--------|---------|--------|
|                  | S 68134                           |        | S 68161 |       | S 68162                           |        | S 68123 |        |
|                  | Centre                            | Edge   | Centre  | Edge  | Centre                            | Edge   | Centre  | Edge   |
|                  | <i>Means of four measurements</i> |        |         |       | <i>Means of four measurements</i> |        |         |        |
| SiO <sub>2</sub> | 39.74                             | 38.76  | 39.76   | 37.91 | 38.87                             | 37.72  | 40.98   | 40.54  |
| FeO              | 21.06                             | 27.26  | 18.33   | 26.02 | 23.94                             | 30.43  | 12.91   | 14.89  |
| MnO              | 0.33                              | 0.52   | 0.23    | 0.34  | 0.61                              | 0.47   | 0.12    | 0.14   |
| MgO              | 40.33                             | 35.62  | 42.51   | 35.59 | 37.93                             | 32.40  | 46.99   | 45.19  |
| NiO              | 0.00                              | 0.00   | 0.00    | 0.00  | 0.00                              | 0.00   | 0.00    | 0.00   |
| Total            | 101.46                            | 102.16 | 100.83  | 99.56 | 101.35                            | 101.02 | 101.00  | 100.76 |
| mg*              | 77.1                              | 69.5   | 80.33   | 70.78 | 73.45                             | 65.15  | 86.53   | 84.28  |

\* mg means  $\frac{\text{Mg}}{\text{Mg} + \text{Fe} + \text{Mn}} \times 100$

S 68134 Tholeiitic dolerite; very coarse grained with ophitic plagioclase and nearly colourless clinopyroxene, minor olivine, skeletal ore, spinel, smectitic mesostasis.

S 68161 Tholeiitic dolerite; plagioclase-phyric with colourless clinopyroxene, very minor olivine, spinel, smectite and granular ore.

S 68162 Crinanitic olivine-dolerite; medium grained, olivine altered partly to smectite, labradorite, purple clinopyroxene, ore, analcime, spinel.

S 68123 Crinanitic olivine-dolerite; olivine-microphyric with labradorite, pale purple clinopyroxene, zeolite, olivine, interstitial analcime, spinel, ore.

Analyst M. T. Styles

**Table 14** Microprobe analyses of feldspar crystals from tholeiitic and crinanitic dykes, Ailsa Craig

|                                | Tholeiitic dykes                  |        |         |        | Crinanitic dykes                  |        |         |       |
|--------------------------------|-----------------------------------|--------|---------|--------|-----------------------------------|--------|---------|-------|
|                                | S 68134                           |        | S 68161 |        | S 68162                           |        | S 68123 |       |
|                                | Centre                            | Edge   | Centre  | Edge   | Centre                            | Edge   | Centre  | Edge  |
|                                | <i>Means of four measurements</i> |        |         |        | <i>Means of four measurements</i> |        |         |       |
| SiO <sub>2</sub>               | 50.98                             | 55.86  | 52.02   | 55.16  | 51.75                             | 56.56  | 51.13   | 54.05 |
| Al <sub>2</sub> O <sub>3</sub> | 31.00                             | 27.44  | 30.28   | 27.58  | 30.09                             | 26.89  | 30.99   | 28.45 |
| Fe <sub>2</sub> O <sub>3</sub> | 0.72                              | 0.98   | 0.84    | 1.00   | 0.66                              | 0.73   | 0.62    | 0.86  |
| CaO                            | 14.70                             | 10.84  | 13.85   | 11.01  | 13.58                             | 9.72   | 14.54   | 11.79 |
| Na <sub>2</sub> O              | 3.06                              | 5.34   | 3.59    | 5.24   | 3.84                              | 6.00   | 3.33    | 4.68  |
| K <sub>2</sub> O               | 0.07                              | 0.14   | 0.12    | 0.14   | 0.00                              | 0.10   | 0.00    | 0.10  |
| Total                          | 100.53                            | 100.60 | 100.70  | 100.13 | 99.92                             | 100.00 | 100.61  | 99.93 |
| An                             | 72.38                             | 52.40  | 67.58   | 53.35  | 66.15                             | 46.90  | 70.70   | 58.03 |
| Ab                             | 27.23                             | 46.78  | 31.78   | 45.85  | 33.85                             | 52.38  | 29.30   | 41.40 |
| Or                             | 0.40                              | 0.81   | 0.68    | 0.80   | 0.00                              | 0.70   | 0.00    | 0.60  |

Analyst M. T. Styles

(20%), up to 10% opaque iron oxide plates, scattered crystals (0.1 mm) of brown spinel, and up to 5% of analcime and fibrous zeolite and chlorite. Cores of plagioclase range up to 82% An, with labradorite to bytownite forming the skeletal or ophitic framework (laths mainly 0.4–0.5 mm long). Augite crystals in thin sections of these rocks are mainly deep to pale purple, plum (also suggesting a crinanitic affinity), zoned in places (colourless to deep purple) skeletal and optically continuous, ophitic with plagioclase and forming ocellar patches (as in S 69762). Olivine crystals are fresh or variably replaced by bowlingite or an orange smectite. Analcime is colourless; interstitial or intersertal, and radially fibrous zeolite (natrolite in S 68124), chlorite and carbonate may occur in amygdales. Opaque iron oxides, usually as plates, form up to 12% by volume in one specimen (S 68162). The two specimens most resembling crinanites (S 68170 and Dollar's dyke No. IV) occur respectively just east of Rotten Nick and just north of Swine Holes. The branch dyke XXXIII occurring at Rotten Nick (XXVII) is not, however, crinanitic and there is no evidence to suggest that the crinanitic variety represents any more than a local enrichment in olivine and accessory analcime/zeolite.

#### MINERALOGY

Two specimens each of the tholeiitic and crinanitic dolerites were analysed on the electron microprobe using the same energy-dispersive X-ray analysis system as for the microgranites.

#### Primary minerals:

**Olivine** The two tholeiitic dykes have similar mean olivine composition (Table 13), with marked zoning from cores around Fo80 to rims around Fo70, but in one crystal to Fo56. The two crinanitic specimens are dissimilar with S 68162 having cores around Fo74 zoned to rims around Fo65 whilst S 68123 shows only slight zoning with cores and rims around Fo85.

**Plagioclase** Both dyke types show similar mean plagioclase compositions, mostly in the labradorite range (Table 14), with cores around An 66–73 and zoned to more sodic rims. In many the rims are in the range 47–58 but others show much more extensive zoning and approach the composition of the interstitial feldspars which are generally more sodic and in S 68162 are around An 13.

**Clinopyroxenes** The clinopyroxenes (Table 15) show the greatest differences between the two types of dyke. The pyroxenes in the tholeiitic dykes are augites that tend to be zoned to more Fe-rich compositions with an average composition around Mg 45, Fe 15 and Ca 40. The Ti content is around 0.02–0.03 formula units (1 wt% TiO<sub>2</sub>) and Al around 0.1–0.15 formula units (2.5–3 wt% Al<sub>2</sub>O<sub>3</sub>). The pyroxenes in the crinanitic dykes are more calcic, either very calcic augites or salites; they show little or no zoning and have an average composition around Mg 36 Fe 18 Ca 46. The Ti content is around 0.7 formula units (2.5 wt% TiO<sub>2</sub>) and Al around 0.2–0.3 formula units (4.5–7.0 wt% Al<sub>2</sub>O<sub>3</sub>).

**Table 15** Electron microprobe analyses of clinopyroxenes from basic dykes, Ailsa Craig

|                                | Tholeiitic dolerites                            |        |         |        | Crinanitic dolerites                            |       |         |        |
|--------------------------------|---|--------|---------|--------|---|-------|---------|--------|
|                                | S 68134   |        | S 68161 |        | S 68162   |       | S 68123 |        |
|                                | Centre  | Edge   | Centre  | Edge   | Centre  | Edge  | Centre  | Edge   |
|                                | <i>Means of four crystals</i>                   |        |         |        | <i>Means of four crystals</i>                   |       |         |        |
| SiO <sub>2</sub>               | 51.22   | 51.20  | 50.85   | 51.03  | 48.53   | 49.10 | 46.99   | 48.71  |
| TiO <sub>2</sub>               | 0.91  | 0.89   | 1.02    | 1.03   | 2.67  | 2.33  | 2.42    | 1.89   |
| Al <sub>2</sub> O <sub>3</sub> | 2.79  | 2.66   | 3.43    | 2.32   | 4.54  | 3.88  | 6.44    | 4.33   |
| Cr <sub>2</sub> O <sub>3</sub> | 0.13  | 0.11   | 0.17    | 0.08   | 0.00  | 0.00  | 0.00    | 0.00   |
| FeO*                           | 9.37  | 10.43  | 10.25   | 13.52  | 10.85   | 10.59 | 11.20   | 13.22  |
| MnO                            | 0.16  | 0.19   | 0.26    | 0.47   | 0.10  | 0.05  | 0.13    | 0.18   |
| MgO                            | 14.98   | 15.22  | 15.26   | 14.27  | 12.50   | 12.36 | 11.22   | 10.36  |
| CaO                            | 19.92   | 18.79  | 18.55   | 16.86  | 20.69   | 20.61 | 21.47   | 20.84  |
| Na <sub>2</sub> O              | 0.31  | 0.52   | 0.44    | 0.49   | 0.77  | 0.59  | 0.75    | 0.82   |
| Total                          | 99.79   | 100.01 | 100.23  | 100.07 | 100.65  | 99.51 | 100.62  | 100.35 |
|                                | <i>Number of ions on the basis of 6 oxygens</i> |        |         |        | <i>Number of ions on the basis of 6 oxygens</i> |       |         |        |
| Si                             | 1.91  | 1.91   | 1.89    | 1.92   | 1.82  | 1.86  | 1.78    | 1.86   |
| Ti                             | 0.02  | 0.02   | 0.03    | 0.03   | 0.08  | 0.06  | 0.07    | 0.05   |
| Al                             | 0.12  | 0.12   | 0.15    | 0.10   | 0.20  | 0.17  | 0.29    | 0.19   |
| Cr                             | 0.01  | 0.01   | 0.01    | 0.01   | 0.00  | 0.00  | 0.00    | 0.00   |
| Fe                             | 0.29  | 0.33   | 0.32    | 0.43   | 0.34  | 0.34  | 0.36    | 0.42   |
| Mn                             | 0.01  | 0.01   | 0.01    | 0.02   | 0.01  | 0.01  | 0.01    | 0.01   |
| Mg                             | 0.83  | 0.85   | 0.84    | 0.80   | 0.70  | 0.70  | 0.63    | 0.59   |
| Ca                             | 0.80  | 0.75   | 0.80    | 0.68   | 0.83  | 0.84  | 0.87    | 0.85   |
| Na                             | 0.02  | 0.03   | 0.03    | 0.04   | 0.05  | 0.04  | 0.05    | 0.06   |
| Mg                             | 43.35   | 44.01  | 44.39   | 41.97  | 37.36   | 37.33 | 34.06   | 31.65  |
| Fe                             | 15.23   | 16.93  | 16.72   | 22.32  | 18.20   | 17.95 | 19.08   | 22.68  |
| Ca                             | 41.43   | 39.07  | 38.89   | 35.72  | 44.45   | 44.73 | 46.87   | 45.72  |
| <u>Mg</u>                      | 74.06   | 72.37  | 72.69   | 65.36  | 67.75   | 67.54 | 64.09   | 58.26  |
| Mg + Fe                        |   |        |         |        |   |       |         |        |

\* Total iron as FeO Analyst M. T. Styles

**Table 16** Electron microprobe analyses of spinels from basic dykes, Ailsa Craig

|  | Tholeiitic dykes             |         | Crinanitic dykes             |         |
|--|------------------------------|---------|------------------------------|---------|
|  | S 68134                      | S 68161 | S 68162                      | S 68123 |
|  | <i>Means of two crystals</i> |         | <i>Means of two crystals</i> |         |
| TiO <sub>2</sub>                             | 18.23                        | 18.56   | 24.90                        | 18.89   |
| Al <sub>2</sub> O <sub>3</sub>               | 3.23                         | 1.50    | 1.69                         | 3.21    |
| Fe <sub>2</sub> O <sub>3</sub> *             | 29.75                        | 28.30   | 17.00                        | 26.00   |
| V <sub>2</sub> O <sub>5</sub>                | NA                           | 0.85    | 0.64                         | 0.66    |
| FeO  | 43.39                        | 47.62   | 51.18                        | 47.59   |
| MnO  | 0.52                         | 0.63    | 0.62                         | 0.70    |
| MgO  | 1.82                         | 1.00    | 2.26                         | 1.24    |
| <i>Total</i>                                 | 96.94                        | 98.46   | 98.29                        | 98.29   |
| <i>Number of ions on basis of 32 oxygens</i> |                              |         |                              |         |
| Ti   | 4.079                        | 4.214   | 5.560                        | 4.249   |
| Al   | 1.131                        | 0.533   | 0.592                        | 1.113   |
| Fe <sup>3+</sup>                             | 6.671                        | 6.419   | 3.799                        | 5.854   |
| V <sup>5+</sup>                              | 0.000                        | 0.000   | 0.152                        | 0.159   |
| Fe <sup>2+</sup>                             | 11.173                       | 12.021  | 12.712                       | 11.902  |
| Mn   | 0.131                        | 0.161   | 0.156                        | 0.177   |
| Mg   | 0.806                        | 0.451   | 1.001                        | 0.550   |

\* Fe<sup>3+</sup> calculated by adjustment of Fe<sup>2+</sup> to give approximately 24 cations

NA Not analysed

*Analyst* M. T. Styles

*Spinel* The spinels from all the rocks are broadly similar (Table 16) titanomagnetites. The Fe<sup>3+</sup> content has been estimated by calculating the ionic formula such that the total number of cations is approximately equal to 24. The spinels all have a high TiO<sub>2</sub> content which produces around 50% of the ulvospinel molecule when the end-member molecules are calculated.

*Late-stage (deuteric) and secondary minerals*

The crinanitic dykes have variably abundant late-stage or alteration minerals, both analcime and zeolites. The

analcimes are very close to an idealised formula (Table 17) and show peripheral alteration to a 'feathery' pale brown mineral that gives a smectite-like composition. The green/brown mesostasis gives compositions that suggest predominant chlorite. The smectites that replace olivine have a wide range of Mg/Fe ratios (Table 17) that bear no relationship to the Mg/Fe ratio of the pre-existing olivine and must be a function of the alteration process. The microprobe analyses, therefore, confirm the petrographic separation of the Ailsa Craig dykes into tholeiitic and crinanitic types. The crinanitic type contains the requisite analcime and also zeolites. They also contain clinopyroxenes that are salitic and with high Ti and Al are typical of basic rocks with alkaline affinities. The Mg-rich olivines, particularly in S 68123, which are more magnesian than the co-existing clinopyroxenes, suggest that they may be xenocrysts that originally crystallised from a more magnesian magma.

*CHEMISTRY*

*Major elements*

Full analyses, by Telsec beta-probe and 'wet-way' methods were made of two samples, one (S 68134) of olivine-poor coarsely ophitic dolerite, with tholeiitic texture, and one of olivine-rich crinanitic dolerite (S 68162) (Table 18, cols. 1 and 2 respectively). Trace elements by Inductively Coupled Plasma Atomic Emission Spectroscopy (ICP) are listed in Table 20; rare earths by neutron activation (Table 21) are normalised to standard chondrite in Figure 4, and trace elements of a third sample, S 68151, an olivine-basalt, analysed by Spark Source Mass Spectrometry, are listed in Table 11 where they are contrasted with those of the Ailsa microgranites. The fully-analysed coarse dolerite (S 68134) is an ophitic mesh of labradorite laths (1.5 mm long) and colourless to very pale brown augite (1 to 2 mm across) with interstitial smaller (0.6 mm) olivine crystals partly altered to a brown clay (? smectite), microcrystalline pale brown clay mesostasis (perhaps representing original glass) and skeletal opaque ore. More tabular plates of plagioclase attain 3 mm across. The crinanitic olivine-dolerite (S 68162) is a much finer subophitic mesh of labradorite laths (0.3 mm long), pale lilac/purple augite (0.2 mm),

**Table 17** Electron microprobe analyses of secondary/late-stage minerals from basic dykes, Ailsa Craig

|                                | Tholeiitic dykes       |                        |          | Crinanitic dykes                   |            |                        |                     |                        |
|--------------------------------|------------------------|------------------------|----------|------------------------------------|------------|------------------------|---------------------|------------------------|
|                                | S 68134                | S 68161                | Analcime | S 68162                            | Mesostasis | S 68123                | Zeolite (scolecite) | S 68123                |
|                                | Smectite after olivine | Smectite after olivine |          | Smectite? - alteration of analcime |            | Smectite after olivine |                     | Smectite after olivine |
| SiO <sub>2</sub>               | 47.30                  | 48.55                  | 55.91    | 56.00                              | 34.12      | 47.13                  | 44.59               | 48.17                  |
| Al <sub>2</sub> O <sub>3</sub> | 4.21                   | 3.68                   | 22.67    | 2.65                               | 12.88      | 4.60                   | 26.64               | 3.65                   |
| FeO                            | 18.20                  | 15.98                  | —        | 4.81                               | 20.84      | 24.79                  | —                   | 12.41                  |
| MnO                            | 0.27                   | 0.33                   | —        | 0.67                               | 0.19       | 0.43                   | —                   | —                      |
| MgO                            | 15.02                  | 14.53                  | —        | 13.19                              | 14.62      | 7.70                   | —                   | 18.83                  |
| CaO                            | 0.53                   | 0.97                   | —        | 0.88                               | 2.79       | 0.58                   | 10.53               | —                      |
| Na <sub>2</sub> O              | 0.39                   | 0.36                   | 12.76    | 0.53                               | 0.57       | 0.48                   | 3.22                | 0.31                   |
| K <sub>2</sub> O               | 1.17                   | 0.92                   | 0.15     | 1.31                               | 0.52       | 1.45                   | —                   | 1.64                   |
| <i>Total</i>                   | 87.09                  | 85.32                  | 91.49    | 80.40                              | 86.53      | 87.16                  | 84.98               | 85.01                  |

— not detected

*Analyst* M. T. Styles

**Table 18** Chemical analyses of basic dykes from Ailsa Craig

|                                | (1)   | (2)   | A      | B     | C      | D         | E         |
|--------------------------------|-------|-------|--------|-------|--------|-----------|-----------|
| SiO <sub>2</sub>               | 48.4  | 46.1  | 47.35  | 46.6  | 48.60  | 46.3-47.8 | 44.6-45.1 |
| Al <sub>2</sub> O <sub>3</sub> | 16.0  | 15.7  | 13.90  | 18.6  | 18.27  | 14-17     | 14-17     |
| Fe <sub>2</sub> O <sub>3</sub> | 3.51  | 4.82  | 5.87   | 3.8   | 3.19   | 10.7-12.6 | 12.4-14.1 |
| FeO                            | 6.99  | 8.64  | 8.96   | 7.5   | 7.17   |           |           |
| MgO                            | 6.93  | 6.69  | 5.97   | 6.7   | 6.29   | 6.9-8.4   | 8.1-10.3  |
| CaO                            | 10.6  | 8.51  | 10.65  | 8.5   | 10.15  | 9.3-10.3  | 8.5-9.2   |
| Na <sub>2</sub> O              | 2.31  | 3.14  | 2.73   | 2.4   | 1.63   | 2.6-3.0   | 3.1-3.4   |
| K <sub>2</sub> O               | 0.30  | 0.23  | 0.54   | 0.4   | 0.45   | 0.3-0.9   | 0.2-0.5   |
| H <sub>2</sub> O <sup>+</sup>  | 1.03  | 1.88  | 1.16   | 1.4   | 1.65   |           |           |
| H <sub>2</sub> O <sup>-</sup>  | 1.57  | 1.05  | 1.04   | 1.9   | 1.60   |           |           |
| CO <sub>2</sub>                | nd    | nd    | 0.32   |       |        |           |           |
| TiO <sub>2</sub>               | 1.02  | 1.86  | 1.75   | 1.9   | 0.70   | 1.4-1.7   | 2.2-2.5   |
| MnO                            | 0.17  | 0.18  | 0.23   | 0.1   | 0.24   |           |           |
| P <sub>2</sub> O <sub>5</sub>  | 0.12  | 0.21  | 0.24   | 0.1   | 0.09   | 0.18-0.25 | 0.25-0.27 |
| S                              |       |       | 0.23   | 0.1   | tr     |           |           |
| Total                          | 98.95 | 99.01 | 100.94 | 100.0 | 100.03 |           |           |

nd Not detected (<0.1% CO<sub>2</sub>)

Major and minor elements determined by  $\beta$ -probe: MnO determined by XRF; H<sub>2</sub>O<sup>+</sup> and H<sub>2</sub>O<sup>-</sup> determined by classical gravimetry.

FeO determined by titrimetry

1 Tholeiitic dolerite, S 68134. Ailsa Craig [NS 0186 0039] Lab. No. 3195

2 Crinanitic alkaline dolerite, S 68162, Ailsa Craig [NX 0221 9927] Lab. No. 3196

A Olivine-tholeiite (Salen Type), dyke 2½ miles NNW of Salen, Mull. *Analyst* F. R. Ennos in Bailey and others, 1924, p. 57

B Olivine-tholeiite (Largs Type), dyke, Creag Bhàn, Allt-Mòr, Whiting Bay, Arran

C Olivine-tholeiite (Corrie Type), Arran. *Analyst* W. H. Herdsman

D Range of hypersthene-normative basalt (Thompson and others, 1972)

E Range of alkali-basalt (Thompson and others, 1972).

*Analysts* A. E. Davis, S. Hobbs and P. T. S. Sandon, Analytical Chemistry Unit, BGS

colourless to altered olivine crystals (0.5 mm) with orange-brown (? smectite) replacements, prominent opaque ore grains, subvesicular patches (to 1.0 mm) of analcime with radial-fibrous zeolite fringes, and other interstitial cryptocrystalline clay material. Modal analyses of these two samples gave in approximate volume per cent:

|         | Plagio-<br>clase | Augite | Olivine (with<br>alteration<br>products) | Ore | Analcime | Meso-<br>stasis |
|---------|------------------|--------|--|-----|----------|-----------------|
| S 68134 | 45               | 38     | 5  | 4   | —        | 8               |
| S 68162 | 38               | 33     | 15                                       | 8   | 1        | 5               |

Despite the differences in mineralogy, the analyses show only a little lower SiO<sub>2</sub>, CaO, K<sub>2</sub>O, higher FeO + Fe<sub>2</sub>O<sub>3</sub>, Na<sub>2</sub>O and TiO<sub>2</sub> in the crinanitic dolerite compared with the tholeiitic dolerite. The higher olivine content of S 68762 is balanced by the higher augite and smectitic mesostasis in S 68134. Generally the two analyses fall within the respective ranges quoted for hypersthene-normative basalt and alkali basalt (Thompson and others, 1972). The crinanitic dolerite matches, except for a little higher Al<sub>2</sub>O<sub>3</sub> (reflecting the higher plagioclase content), olivine-'tholeiite' (Salen Type) from Mull (Table 18, analysis A) and (except for lower Al<sub>2</sub>O<sub>3</sub>), the recalculated carbonate-free analysis (Table 18, analysis B) of olivine-'tholeiite' (Largs type) from Arran.

**Table 19** Norms of basic dykes

|                       | S 68134             |       | S 68162                      |       |
|-----------------------|---------------------|-------|------------------------------|-------|
|                       | Tholeiitic dolerite |       | Crinanitic alkaline-dolerite |       |
|                       | (a)                 | (b)   | (a)                          | (b)   |
| Q                     | 1.44                | 0.00  | 0.00                         | 0.00  |
| Ab                    | 20.26               | 20.50 | 27.61                        | 28.15 |
| Or                    | 1.84                | 1.86  | 1.41                         | 1.44  |
| An                    | 33.64               | 34.03 | 29.21                        | 29.77 |
| Di                    | 16.26               | 16.61 | 10.54                        | 10.90 |
| Hy                    | 18.93               | 22.01 | 14.08                        | 9.81  |
| Ol                    | 0.00                | 0.34  | 5.56                         | 13.21 |
| Mt                    | 5.28                | 2.28  | 7.27                         | 2.31  |
| Il                    | 2.01                | 2.03  | 3.68                         | 3.75  |
| Ap                    | 0.29                | 0.29  | 0.60                         | 0.61  |
| Total                 | 99.96               | 99.96 | 99.95                        | 99.96 |
| Agpaicity coefficient | 0.26                | 0.26  | 0.34                         | 0.34  |
| Differentiation index | 23.54               | 22.36 | 29.02                        | 29.59 |

All norms quoted in weight per cent

(a) Analyses from Table 18

(b) As (a) but Fe<sub>2</sub>O<sub>3</sub> standardised to 1.50

**Table 20** Trace elements of basic dykes (ppm) (*see also* Table 16)

| Group       |    | Tholeiitic dolerite | Crinanitic alkaline dolerite |
|-------------|----|---------------------|------------------------------|
| <b>IA</b>   | Rb | 5                   | 0                            |
| <b>IB</b>   | Cu | 76                  | 75                           |
| <b>IIA</b>  | Sr | 165                 | 260                          |
| <b>IIB</b>  | Zn | 73                  | 78                           |
| <b>IIIA</b> | B  | <10                 | <10                          |
| <b>IIB</b>  | Y  | 25                  | 25                           |
|             | La | 10                  | 10                           |
|             | Ce | 13                  | 15                           |
| <b>IVB</b>  | Zr | 71                  | 133                          |
| <b>VA</b>   | As | 0                   | 1                            |
| <b>VB</b>   | V  | 230                 | 190                          |
|             | Nb | 2                   | 2                            |
| <b>VIB</b>  | Cr | 100                 | 140                          |
| <b>VIII</b> | Co | 59                  | 81                           |
|             | Ni | 96                  | 130                          |

Tholeiitic dolerite, S 68134, Ailsa Craig [NS 0186 0039] Lab. No. 3195

Crinanitic alkaline dolerite, S 68162, Ailsa Craig [NX 0221 9927]. Lab. No. 3196

*Analysts* T. K. Smith, M. Ingham and B. A. R. Tait. Analytical Chemistry Unit, BGS. Elements determined by Inductively Coupled Plasma Atomic Emission Spectroscopy (except B, by XRF).

These olivine-dolerites show affinities with the Staffa types amongst the basalt lavas of the Western Isles, and with the non-porphyrific central-basalt magma type of Mull in general (Tyrrell, 1928). The norm of S 68162, however, shows no excess silica and is not magmatically oversaturated. The tholeiitic dolerite (S 68134) on the other hand contains 1.44% excess SiO<sub>2</sub> and its analysis matches (except for lower Al<sub>2</sub>O<sub>3</sub> and slightly higher

**Table 21** Neutron activation analyses of dolerites for rare earths and other trace elements

|               | La   | Ce   | Nd   | Sm   | Eu   | Tb   | Ho   | Yb   | Lu    | Ta   | Th   | U    | Hf   | W  |
|---------------|------|------|------|------|------|------|------|------|-------|------|------|------|------|----|
| Atomic weight | 57   | 58   | 60   | 62   | 63   | 65   | 67   | 70   | 71    | 73   | 90   | 92   | 72   | 74 |
| S 68134       | 4.62 | 15.4 | 8.8  | 3.01 | 1.11 | 0.66 | 1.1  | 2.31 | 0.358 | 0.42 | 0.70 | 0.21 | 2.18 | 34 |
| S 68162       | 4.61 | 22.9 | 15.6 | 4.84 | 1.81 | 0.84 | 0.85 | 2.22 | 0.358 | 0.65 | <0.7 | <1.2 | 3.77 | 41 |

*Analyst* Dr Susan Parry, University of London Reactor Centre, Silwood Park, Ascot, Berkshire

Na<sub>2</sub>O) olivine-tholeiite of Corrie type (Table 18, analysis C) which Tyrrell (1928) notes resembles the porphyritic central-magma type of Mull. The tholeiitic dolerite significantly contains no normative olivine (or only 0.34% when the Fe<sub>2</sub>O<sub>3</sub> is standardised to 1.5%) compared with 5.56% (13.21% likewise standardised) olivine in the crinanitic dolerite.

Though the Ailsa dykes do not include representatives of the more SiO<sub>2</sub>-oversaturated tholeiites (quartz-dolerites), they do show two moderately distinct varieties, one corresponding to the olivine-basalts, olivine-dolerites and crinanites of plateau-basalt type of Mull, and the other to the porphyritic central-magma type, that is, approaching the more basic types of the quartz-dolerite/tholeiite group. In terms of the tholeiite trend on the FMA diagram, however, both of the analysed dolerites plot closely towards the peak of Fe-enrichment – which distinguishes the tholeiitic from the calc-alkali trend. On the total alkalis: silica diagram, the tholeiitic dolerite and the crinanitic dolerite fall in the subalkaline and alkaline basalt fields respectively (Irvine and Baragar, 1971).

#### *Trace-element geochemistry (whole-rock)*

The trace elements (Tables 20; 21; Figure 4) fall within the ranges for basic rocks and there are no anomalous values. When the two dolerites are compared, Co, Cr and Ni are higher in the crinanitic dolerite as are the incompatible elements Zr, Ti, P and most of the rare earths (except Ho, Yb). When the two dolerites are compared with the Ailsa microgranite (Table 11) most elements have considerably higher ranges in the latter except (as would be expected on geochemical grounds) Cu and S. The compatible elements Ni, Cr, Co are not quoted for the microgranites but these are probably much lower than the values found for the dolerites (Table 20), which are about average for basic rocks. The rare earth elements for the dolerites, normalised to standard chondrite (Figure 4), show a slight depletion in La, but otherwise a relatively smooth decrease to the HREE. The REEs are considerably enriched in the microgranites except for the pronounced negative Eu anomaly which coincides in value with that for the crinanitic dolerite (S 68162) though this probably has no genetic implication.

#### *METAMORPHISM OF THE MICROGRANITE BY DYKE INTRUSION*

Effects of the emplacement of dykes on the petrography and the mineralogy of the adjacent microgranite have been minimal. Sections (S 72795, 72794) through microgranite/dyke contacts show only a slight diminution in grain size within a mm or so of the contact in both rocks. Along some contacts ferric oxide is extensively developed.

## DISCUSSION

### *PETROGENESIS*

Textural variations in the Ailsa Craig microgranite, principally the markedly fine-grain size in the upper and north-eastern parts of the island, suggest that these parts of the island are proximal to original country rock contacts. The present morphology of the island, with the exception of the western and southern faces which are clearly more prone to marine denudation, probably represents the original form of the intrusion, with all covering country rocks since removed. Based on as representative sampling as possible, within limited textural variations the microgranite is chemically and mineralogically homogeneous and represents a single major intrusive phase. The dolerite dykes are completely unrelated mineralogically and chemically to the microgranite and the only effects of their emplacement have been a sporadic dissemination of Fe<sub>2</sub>O<sub>3</sub> (mainly as hematite) into the wall-rocks, and a slight sintering of the microgranite at the actual contact. The chilled margins of the dykes themselves show basaltic textures and have been affected by alteration to clay material of the ferromagnesian minerals. The chilled margins, the sharp contacts, and relation of dyke intrusions to the major joint systems of the microgranite, all clearly prove that the latter was cold and solid during emplacement of the dyke magma.

The genesis of the acid magmas of the British Tertiary Province remains highly controversial, with opinion divided between crustal melting (anatexis) with all degrees of partial melting, and differentiation from a basaltic magma. Meighan (1979) summarises these proposals with an extensive bibliography, but suggests differentiation of basaltic magmas of variable starting compositions as the more likely process. Though Ailsa Craig is, by comparison with other Tertiary acid bodies, volumetrically very small, nevertheless only very minor and sporadic xenoliths of sedimentary rocks occur and have only very locally affected this homogeneous intrusion in mineralogy and chemistry. To this extent, Ailsa is similar to other acid intrusions of the Province. Meighan (1979) notes 'So far no Tertiary acid intrusion has been found to show marked chemical inhomogeneity attributable to its having crystallised from an unhomogenised partial melt of source-rocks'. Remelting of older granites is unlikely since, according to Meighan, none of the Tertiary granites has trace element compositions (such as high Sr—Ailsa has less than 3 ppm Sr) compatible with total melting of typical Caledonian granodiorites, none of which in any case underlies these Tertiary centres so far as is known. On the contrary, the very low Sr, high Zr (60–1500 ppm), LREE and negative Eu anomaly all support an origin through differentiation of tholeiitic basic magmas.

The alkaline acid rocks, including Ailsa Craig, Holy

Island, and Rockall, are volumetrically very minor parts of the Tertiary acid province. Meighan cites biotite-granites, formed through extreme differentiation of subalkaline granite magma in the eastern Mourne Mountains and which contain considerably more Rb and less Zr than the Ailsa Craig microgranite and the other alkaline granitic intrusions, as evidence against the latter being formed by such differentiation. Further he considers it unlikely that the Ailsa microgranite acquired its distinctive mineralogy and chemistry through interaction of an earlier solidified subalkaline microgranite and a Tertiary hydrothermal-meteoric or other metasomatic system (see Beckinsale, 1974). Meighan (1979) suggests that through differentiation (that is, feldspar-fractionation accounting for the negative Eu anomaly) of basaltic magmas of variable composition, occurring in upper crustal magma chambers, the complex acid–basic magma coexistence can be explained as early acid derivatives of parental basic magmas followed by later acid pulses forming the basic dykes of Ailsa and elsewhere. This hypothesis may also indicate the origin of a range of granitic compositions, from subalkaline to peralkaline. The apparent scarcity of intermediate rocks has long suggested independent partial melting of the upper mantle (to produce basic magma) and continental crust (to produce acid magma). But Meighan (1979) considers that this apparent scarcity may only be a function of the present erosional level and that such intermediate rocks may be present at greater depths.

Since Ailsa lies so close, and is of similar age, to the far greater and more diversified Tertiary Complex of Arran, discussion of the origin of the latter centre is most relevant to that of Ailsa. Dickin and others (1981) in a geochemical study of the relatively small number (38) of samples, consider (after Tyrrell, 1928) that the basic rocks define two separate lineages on oxide-variation diagrams—one crinanitic (silica-undersaturated, alkali-enriched) and the other craignuritic (silica-oversaturated). But values of the acid intrusives are colinear with those of the oversaturated basic rocks. The Holy Island trachyte, which is compared with the Ailsa microgranite, is much less silica-saturated than the granites of Arran. Dickin and others (1981) consider that the trachyte is probably 'a product of extensive differentiation and late-stage silica-enrichment of a magma resembling the composition of the.... (crinanite) sills'.

Initial Sr ratio (at age 59 Ma) for the Tertiary igneous rocks of Arran (Dickin and others, 1981) range from 0.7032 for the undersaturated suite to 0.7186 for the Northern Granite. They do not indicate anatexis of Dalradian, New Red or Old Red Sandstones though anatexis of Lewisian basement (with  $^{87}\text{Sr}/^{86}\text{Sr} = 0.702$  to 0.730 at 59 Ma) may have occurred to form the granites of Arran. However, the  $^{87}\text{Sr}/^{86}\text{Sr}$  ratio for the Holy Island intrusion (0.70658) barely supports such a process. Lead isotope measurements by Dickin and others (1981) do not indicate genesis of the Arran Tertiary rocks by anatexis of Lewisian gneiss.

The initial  $^{87}\text{Sr}/^{86}\text{Sr}$  ratio of  $0.7028 \pm .0009$  for the Ailsa microgranite (this paper) is significantly lower than that of the nearby Holy Island trachyte but strongly indicates a complete lack of anatexis of any underlying continental crust—whether Lewisian, Dalradian, Old Red or New Red Sandstone. On the contrary, the new data strongly support derivation through fractionation directly from a primitive mantle-derived magma and along an initially undersaturated trend. The reason for absence of anatexis or of continental crustal contamination for a small body remote from the oceanic/continental crustal

margin (western margin of the north-west European shelf) is most intriguing, but cannot be considered here out of context of a review of the Tertiary magmatic provinces as a whole. Though the dykes intrude the microgranite, they probably arose as pulsed injections of basic magma as silica-saturated or slightly undersaturated crinanitic types from chambers isolated from those which supplied the granite magma.

## ACKNOWLEDGEMENTS

Apart from the contributors and the acknowledgements made in the Preface, the authors are indebted to many colleagues and friends for their assistance: to Mrs Jenny Dollar for a collection of her late husband's maps, specimens, notes and photographs (deposited with the British Geological Survey, and the Hunterian Museum, Glasgow), to Professor R. A. Howie and Mr F. J. Fitch for helpful discussions, to Mr C. W. Wheatley and Mr R. D. Fakes for preparing many thin and polished sections. In our search for information on the suspected occurrence of gold in the Ailsa microgranite, we are very indebted to Dr C. D. Waterston of the Royal Scottish Museum, Edinburgh, Mr J. Hunter (Curator) and Mr C. Woodward of the Dick Institute, Kilmarnock, and to Dr J. D. Bignell of Warren Spring Laboratory, for flotation separations.

## REFERENCES

- ANONYMOUS. 1941. Account of paper read by Dr A. T. J. Dollar on Ailsa Craig, to the Royal Society of Edinburgh. In *The Scotsman and the Glasgow Herald*, 14.1.1941.
- 1961. Ailsa Craig Quarry reopened to meet demand for curling stones. *Quarry Managers Journal*, Vol. 45, 404–405.
- BAILEY, E. B., CLOUGH, C. T., WRIGHT, W. B., RICHEY, J. E. and WILSON, G. V. 1924. Tertiary and post-Tertiary Geology of Mull, Loch Aline, and Oban. *Mem. Geol. Surv. G.B.*
- BAMFORD, D. 1979. Seismic constraints on the deep geology of the Caledonides of northern Britain. Pp. 93–96 in HARRIS, A. L., HOLLAND, C. H. and LEAKE, B. E. (Eds.) *The Caledonides of the British Isles — reviewed*. (Edinburgh: Scottish Academic Press.)
- BECKINSALE, R. D. 1974. Rb-Sr and K-Ar age determinations and oxygen isotope data for the Glen Cannel Granophyre, Isle of Mull, Argyllshire, Scotland. *Earth Planet. Sci. Lett.*, Vol. 22, 267–274.
- BOULDER COMMITTEE. 1884. Tenth and final report. *Proc. Roy. Soc. Edinburgh*, Vol. 12, 765–926.
- BUCKLEY, H. A., BEVAN, J. C., BROWN, K. M., JOHNSON, L. R. and FARMER, V. C. 1978. Glauconite and celadonite: two separate mineral species. *Mineral. Mag.*, Vol. 42, 373–382.
- CHARLESWORTH, J. K. 1957. *The Quaternary Era*, Vol. I, 368–369. (London: Edward Arnold.)
- CORKEY, W. 1937. Ailsa erratic in County Donegal. *Irish Nat. J.*, Vol. 6, 178.
- DAGLEY, P., MUSSETT, A. E., WILSON, R. L. and HAIL, J. M. 1978. The British Tertiary igneous province: palaeomagnetism of the Arran Dykes. *Geophys. J. R. Astr. Soc.*, Vol. 54, 75–91.
- DEARNLEY, R. 1979. Image analysis — some applications to Tertiary minor intrusions. *Bull. Geol. Surv. G.B.*, No. 70, 23–33.

- DICKIN, A. P., MOORBATH, S. and WELKE, H. J. 1981. Isotope, trace element and major element geochemistry of Tertiary igneous rocks, Isle of Arran, Scotland. *Trans. Roy. Soc. Edinburgh*, Vol. 72, 159–170.
- EVANS, A. L., FITCH, F. J. and MILLER, J. A. 1973. Potassium-argon age determinations on some British Tertiary igneous rocks. *J. Geol. Soc. London*, Vol. 129, 419–444.
- EVANS, D., CHESHER, J. A., DEEGAN, C. E. and FANNIN, N. G. T. 1982. The offshore geology of Scotland in relation to the IGS shallow Drilling Programme, 1970–1978. *Rep. Inst. Geol. Sci.*, No. 81/12. 36 pp.
- EVANS, J. W. 1925. Regions of Tension. Anniversary address of the President. *Q. J. Geol. Soc. London*, Vol. 81, lxxx–cxxii.
- GEOLOGICAL SURVEY OF SCOTLAND 1869. Explanation of sheet 7: Ayrshire: South-Western District. *Mem. Geol. Surv. G.B.*
- GRAHAM, A. M. and UPTON, B. G. J. 1978. Gneisses in diatremes, Scottish Midland Valley; petrology and tectonic implications. *J. Geol. Soc. London*, Vol. 135, 219–228.
- HARDING, R. R. 1983. Zr-rich pyroxenes and glaucophanic minerals in the Tertiary alkali granite of Ailsa Craig. *Scott. J. Geol.*, Vol. 19, 219–227.
- MERRIMAN, R. J. and NANCARROW, P. H. A. 1984. St Kilda: an illustrated account of its geology. *Rep. Br. Geol. Surv.*, Vol. 16, No. 7.
- HASKIN, L. A. 1979. On rare-earth element behaviour in igneous rocks. Pp. 175–189 in AHRENS, L. H. (Ed.). *Origin and distribution of the elements. Phys. Chem. of the Earth*, Vol. 11. (London: Pergamon Press.) 2nd symp. on the origin and distribution of the elements. Paris, 1977.
- HASKIN, M. A., FREY, F. A. and WILDEMAN, T. R. 1968. Relative and absolute terrestrial abundances of the rare-earth elements. Pp. 830–911 in AHRENS, L. H. (Ed.) *Origin and distribution of the elements*. (London: Pergamon.) Symposium on the origin and distribution of the elements, Paris, 1967.
- HAWKES, J. R. 1975. Rockall Island: new geological, petrological, chemical and Rb-Sr age data. Pp. 15–49 in HARRISON, R. K. (Ed.) *Expedition to Rockall, 1971–1972. Rep. Inst. Geol. Sci.*, No. 75/1.
- HEDDLE, M. F. 1897. On the crystalline forms of riebeckite. *Trans. Edinburgh Geol. Soc.*, Vol. 7, 265–267.
- HEDDLE, M. F. 1901. *The mineralogy of Scotland*, Vols. I and II. (Edinburgh: D. Douglas.)
- HOWIE, R. A. and WALSH, J. N. 1981. Riebeckitic arfvedsonite and aenigmatite from the Ailsa Craig microgranite. *Scott. J. Geol.*, Vol. 17, 123–128.
- HUSH, J. S. 1970. The case of the clean cut curling stone. *Ind. Diamond Rev.*, Nov. 1970, 440–448.
- IRVINE, E. T. N. and BARAGAR, W. R. A. 1971. A guide to the chemical classification of the common volcanic rocks. *Can. J. Earth Sci.*, Vol. 8, 523–548.
- JARDINE, W. G. 1971. Form and age of Late Quaternary shorelines and coastal deposits of south-west Scotland: critical data. *Quaternaria*, Vol. 14, 103–114.
- JEHU, T. J. 1904. The glacial deposits of northern Pembrokeshire. *Trans. Roy. Soc. Edinburgh*, Vol. 41, 53–88.
- KENDALL, P. F. 1891. On the source of some remarkable boulders in the Isle of Man. *Proc. Manchester Lit. Phil. Soc.*, Vol. 4, 217–220.
- LACROIX, A. 1923. La constitution du banc de Rockall. *C. R. Acad. Sci.*, Vol. 177, 437–440.
- LAWSON, R. 1895. *Ailsa Craig, its history and natural history*. (Paisley: J. and R. Parlanc.) 90 pp.
- MACARTNEY, W. N. 1869. The geology of Ailsa Craig. *Proc. Nat. Hist. Soc. Glasgow*, Vol. 1, 151–157.
- MACINTYRE, R. M. 1973. Lower Tertiary geochronology of the north Atlantic Continental margins. Pp. K1–K25 in PIDGEON, R. T., MACINTYRE, R. M., SHEPPARD, S. M. F. and VAN BREEMEN, O. *Geochronology and isotope geology of Scotland: field guide and reference*. East Kilbride: Scottish Universities Research and Reactor Centre, Isotope Geology Unit.
- MCMENAMIN, T. and PRESTON, J. 1975. K-Ar results from western Ireland and their bearing on the timing and siting of Thulean magmatism. *Scott. J. Geol.*, Vol. 11, 227–249.
- MACKIE, W. J. 1928. The heavier accessory minerals in the granites of Scotland. *Trans. Geol. Soc. Edinburgh*, Vol. 12, 22–40.
- MCLEAN, A. C. and WREN, A. E. 1978. Gravity and magnetic studies of the lower Firth of Clyde. Pp. 7–27 in MCLEAN, A. C. and DEEGAN, C. E. (Eds.) *The solid geology of the Clyde Sheet (55°N/6°W). Rep. Inst. Geol. Sci.*, No. 78/9.
- MEIGHAN, I. 1979. The acid igneous rocks of the British Tertiary Province. *Bull. Geol. Surv. G.B.*, No. 70, 10–22.
- MURATA, K. J. and BASTRON, H. 1956. Convenient method for recognising non-opaque cerium minerals. *Science*, Vol. 123, No. 3203, 888–889.
- PENN, I. E., HOLLIDAY, D. W., KIRBY, G. A., KUBALA, M., SOBEY, R. A., MITCHELL, W. I., HARRISON, R. K. and BECKINSALE, R. D. 1983. The Larne No. 2 Borehole: discovery of a new Permian volcanic centre. *Scott. J. Geol.*, Vol. 19, 333–346.
- ROBERT, J. L. and MAURY, R. C. 1979. Natural occurrence of (Fe, Mn, Mg) tetrasilicic potassium mica. *Contrib. Min. Pet.*, Vol. 68, 117–123.
- SABINE, P. A. 1960. The geology of Rockall, North Atlantic. *Bull. Geol. Surv. G.B.*, No. 16, 156–178.
- SISSONS, J. B. 1974. The Quaternary in Scotland: a review. *Scott. J. Geol.*, Vol. 10, 311–337.
- SMITH, D. B., BRUNSTROM, R. G. W., MANNING, P. I., SIMPSON, S. and SHOTTON, F. W. 1974. A correlation of Permian rocks in the British Isles. *Spec. Rep. Geol. Soc. London*, No. 5, 22–25.
- SMITH, J. V. 1974. *Feldspar minerals. I Crystal structure and physical properties*. (Berlin, Heidelberg and New York: Springer-Verlag.) 627 pp.
- TATEYAMA, H., SHIMODA, S. and SUDO, T. 1974. The crystal structure of synthetic Mg<sup>IV</sup> mica. *Z. Krist.*, Vol. 139, 196–206.
- TEALL, J. J. H. 1891. On a microgranite containing riebeckite from Ailsa Craig. *Mineral. Mag.*, Vol. 9, 219–221.
- THOMPSON, R. N., ESSON, J. and DUNHAM, A. C. 1972. Major element variation in the Eocene lavas of the Isle of Skye, Scotland. *J. Petrol.*, Vol. 13, 219–253.
- TUREKIAN, K. K. and WEDEPOHL, K. H. 1961. Distribution of the elements in some major units of the Earth's crust. *Bull. Geol. Soc. Am.*, Vol. 72, 175–192.

- TYRRELL, G. W. 1928. Geology of Arran. *Mem. Geol. Surv. G.B.*, 237-255.
- UPTON, B. G. J., ASPEN, P., GRAHAM, A. and CHAPMAN, N. A. 1976. Pre-Palaeozoic basement of the Scottish Midland Valley. *Nature, London*, Vol. 260, 517-518.
- VEVERS, H. G. 1936. The land vegetation of Ailsa Craig. *J. Ecol.*, Vol. 24, 424-445.
- WALKER, G. P. L. 1979. The environment of Tertiary igneous activity in the British Isles [Abs.]. *Bull. Geol. Surv. G.B.*, No. 70, 5-6.
- WARRINGTON, G. 1973. Miospores of Triassic age and organic-walled microplankton from the Auchenhew Beds, south-east Arran. *Scott. J. Geol.*, Vol. 9, 109-116.
- YORK, D. 1967. The best isochron. *Earth Planet. Sci. Lett.*, Vol. 2, 479-482.

## APPENDIX

Froth flotation of microgranite samples for suspected precious metals

by Dr J. D. Bignell\*

Two samples (S 68131, 68136) were bulked, well mixed together and riffled to give two subsamples. Both were ground for 20 minutes in a rod mill with 95% passing 125  $\mu\text{m}$ -mesh sieve. The first subsample was froth-floated to give rougher and scavenger concentrates, and tailings. Slime was decanted from the rougher concentrate; slime and sand subsamples were dried and recombined. The second subsample was leached with cyanide for 24 hours and assayed, but with negative results. The rougher and scavenger concentrates were later analysed by Dr Susan Parry† by neutron activation and gave:

|                      |                       | Au (ppm) | Ag (ppm) |
|----------------------|-----------------------|----------|----------|
| S 68131              | Scavenger concentrate | 0.21     | 3.9      |
| <i>combined with</i> |                       |          |          |
| S 68136              | Rougher concentrate   | 0.65     | 9.7      |

\* Mineral Processing Division, Warren Spring Laboratory, Stevenage, Hertfordshire

† University of London Reactor Centre, Silwood Park, Ascot, Berkshire



#### **BRITISH GEOLOGICAL SURVEY**

Keyworth, Nottingham NG12 5GG  
Murchison House, West Mains Road,  
Edinburgh EH9 3LA

The full range of Survey publications is available through the Sales Desks at Keyworth and Murchison House. Selected items are stocked by the Geological Museum Bookshop, Exhibition Road, London SW7 2DE; all other items may be obtained through the BGS London Information Office in the Geological Museum. All the books are listed in HMSO's Sectional List 45. Maps are listed in the BGS Map Catalogue and Ordnance Survey's Trade Catalogue. They can be bought from Ordnance Survey Agents as well as from BGS.

*The British Geological Survey carries out the geological survey of Great Britain and Northern Ireland (the latter as an agency service for the government of Northern Ireland), and of the surrounding continental shelf, as well as its basic research projects. It also undertakes programmes of British technical aid in geology in developing countries as arranged by the Overseas Development Administration.*

*The British Geological Survey is a component body of the Natural Environment Research Council.*

Maps and diagrams in this book use topography based on Ordnance Survey mapping

#### **HER MAJESTY'S STATIONERY OFFICE**

HMSO publications are available from:

##### **HMSO Publications Centre**

(Mail and telephone orders)

PO Box 276, London SW8 5DT

Telephone orders (01) 622 3316

General enquiries (01) 211 5656

*Queueing system in operation for both numbers*

##### **HMSO Bookshops**

49 High Holborn, London WC1V 6HB

(01) 211 5656 (Counter service only)

258 Broad Street, Birmingham B1 2HE

(021) 643 3740

Southey House, 33 Wine Street, Bristol BS1 2BQ

(0272) 264306

9 Princess Street, Manchester M60 8AS

(061) 834 7201

80 Chichester Street, Belfast BT1 4JY

(0232) 238451

71 Lothian Road, Edinburgh EH3 9AZ

(031) 228 4181

##### **HMSO's Accredited Agents**

(see Yellow Pages)

*And through good booksellers*